

# 1 **Extreme floods of Venice: characteristics, dynamics, past and** 2 **future evolution** (review article)

3  
4  
5 Piero Lionello<sup>1</sup>, David Barriopedro<sup>2</sup>, Christian Ferrarin<sup>3</sup>, Robert J. Nicholls<sup>5</sup>, Mirko Orlic<sup>4</sup>, Fabio  
6 Raicich<sup>6</sup>, Marco Reale<sup>7</sup>, Georg Umgiesser<sup>3,10</sup>, Michalis Vourdoukas<sup>8</sup>, Davide Zanchettin<sup>9</sup>

7  
8 <sup>1</sup>University of Salento, DiSTeBA - Department of Biological and Environmental Sciences and Technologies, via per  
9 Monteroni, 165, Lecce, Italy and EuroMediterranean Center on Climate Change

10 <sup>2</sup>Instituto de Geociencias (IGEO), CSIC-UCM, C/Doctor Severo Ochoa 7, 28040 Madrid, Spain

11 <sup>3</sup>CNR - National Research Council of Italy, ISMAR - Marine Sciences Institute, Castello 2737/F, 30122, Venezia, Italy

12 <sup>4</sup>Department of Geophysics, Faculty of Science, University of Zagreb, Croatia

13 <sup>5</sup>Tyndall Centre for Climate Change Research, University of East Anglia, Norwich NR4 7TJ, United Kingdom

14 <sup>6</sup>CNR, Institute of Marine Sciences, AREA Science Park Q2 bldg., SS14 km 163.5, Basovizza, 34149 Trieste, Italy

15 <sup>7</sup> National Institute of Oceanography and Applied Geophysics – OGS and Abdus Salam ICTP, via Beirut 2-4, Trieste,  
16 Italy

17 <sup>8</sup>European Commission, Joint Research Centre (JRC), Ispra, Italy

18 <sup>9</sup>University Ca' Foscari of Venice, Dept. of Environmental Sciences, Informatics and Statistics, Via Torino 155, 30172  
19 Mestre, Italy

20 <sup>10</sup> Marine Research Institute, Klaipeda University, Klaipeda, Lithuania

21  
22  
23 *Correspondence to:* Piero Lionello ([piero.lionello@unisalento.it](mailto:piero.lionello@unisalento.it))

## 24 **Abstract**

25 Floods in the Venice city centre result from the superposition of several factors: astronomical tides, seiches and  
26 atmospherically-forced fluctuations, which include storm surges, meteotsunamis, and surges caused by atmospheric  
27 planetary waves. All these factors can contribute to positive sea-level/water-height anomalies individually and can also  
28 result in/increase the probability of extreme sea-level-events when they act constructively. The largest extreme sea  
29 level/water heights-events are mostly caused by the storm surges produced by the Sirocco winds. This leads, leading to a  
30 characteristic seasonal cycle, with the largest and most frequent events occurring from November to March. Storm surges  
31 can be produced by cyclones whose centres are located either north or south of the Alps. Historically, the most intense  
32 events have been produced by cyclogenesis in the western Mediterranean, to the west of the main cyclogenetic area of  
33 the Mediterranean region in the Gulf of Genoa. Only a small fraction of the interannual variability of extreme sea  
34 levels/water heights is described by fluctuations in the dominant patterns of atmospheric circulation variability over the  
35 Euro-Atlantic sector. Therefore, decadal fluctuations of sea-level/water-height extremes remain largely unexplained. In  
36 particular, the effect of the 11-year solar cycle does not appear to be steadily present if more than one hundred years of  
37 observations are considered. appears to be small, non-stationary or masked by other factors. The historic increase in the  
38 frequency of extreme-sea-levels/floods since the mid-19<sup>th</sup> century is explained by relative mean sea-level rise, with no  
39 long-term trend in the intensity of the atmospheric forcing. Analogously, future regional relative mean sea-level rise will  
40 be the most important driver of increasing duration and intensity of Venice floods through this century, overwhelming  
41 overcompensating for the small projected decrease in of marine storminess projected during the 21 century. Consequently,

42 ~~†~~The future increase of extreme ~~sea level~~water heights covers a ~~large wide~~ range, ~~partly largely~~ reflecting the highly  
43 uncertain mass contributions to future mean sea ~~level~~ rise from the melting of Antarctica and Greenland ice-sheets,  
44 especially towards the end of the century. ~~In conclusion, †~~For a high emission scenario (RCP8.5), the magnitude of 1-  
45 in-100 year ~~sea level~~water-height events-values at the North Adriatic coast is projected to increase ~~up to 65% by 26-35~~  
46 ~~cm and 160%~~ in 2050 ~~and by 53-171 cm and in~~ 2100, ~~respectively,~~ with respect to the present value, and subject to  
47 continued increase thereafter. ~~For a moderate emission scenario (RCP4.5), these values are 12-17cm in 2050 and 24-~~  
48 ~~56cm in 2100.~~ Local subsidence (which is not included in these estimates) ~~will~~can further contribute to the future increase  
49 of extreme ~~sea level~~water heights. This analysis shows the need for adaptive long term planning of coastal defenses ~~with~~  
50 using flexible solutions that are appropriate across the ~~can be adopted to face the~~ large range of plausible future ~~sea-~~  
51 ~~level~~water-height extremes.

52 **key words:** Venice, extreme events, floods, relative sea level rise, surges, climate change, trends

### 53 1. Introduction

54 This paper reviews current understanding ~~on the extreme water level~~of the factors that are responsible for the damaging  
55 floods affecting the Venice city ~~center~~centre and for their future evolution. ~~†~~Such as the event ~~on of~~ 4<sup>th</sup> November 1966,  
56 ~~which produced with~~ estimated damages of 400 million euros (De Zolt *et al.*, 2006), ~~or the event on and of~~ 12 November  
57 2019 (Cavaleri *et al.*, 2020), with estimated damages of 460 million euros<sup>1</sup> and extensive global media coverage, highlight  
58 the risks that ~~Future extreme floods could produce dramatic damages and losses of a unique monumental and cultural~~  
59 ~~heritage bring.~~ Potential damages have often been linked to future relative sea level (RSL) rise. ~~They have been~~  
60 ~~estimated~~Costs of 7 billion euros have been estimated by the mid of this century if relative sea level rise RSL (RSL) rise  
61 continues at the rate observed ~~rate for in~~ the 20th century (an unrealistic scenario based on recent trends and model  
62 projections) and can reach 8 and 16 billion euros for severe and high-end RSL rise scenarios, respectively (Caporin and  
63 Fontini, 2016). These estimates ignore adaptation options, ~~but~~ ~~However, they~~ show the large exposure and the values at  
64 stake. In order to prevent damages and losses of a unique monumental and cultural heritage, in 1994 the Italian  
65 government approved the construction of a system of mobile barriers (MoSE, Modulo Sperimentale Elettromeccanico)  
66 to prevent the flooding of Venice ~~during high sea level events~~. MoSE's construction was initiated in 2003 and it has been  
67 successfully tested in October 2020.

68 The understanding of the dynamics leading to extreme ~~water level~~ floods and of the future evolution of their height and  
69 frequency is of paramount importance for ~~an accurate realistic~~ assessment of present and future risks. This ~~can provide~~  
70 information is needed for efficient management of the implemented defence systems (see also Umgiesser *et al.*, 2021<sup>10</sup>,  
71 in this special issue), the assessing assessment of their effectiveness in ~~the framework of the future increase of extreme~~  
72 ~~sea levels from a climate change perspective and the development of the development of~~ new strategies to cope with  
73 future scenarios (see also Zanchettin *et al.*, 2020, and Lionello *et al.*, 2020 in this special issue).

74 The city of Venice is located in the centre of a large and shallow lagoon (Fig. 1), covering 500 km<sup>2</sup> with an average depth  
75 of about 1 m. Water is exchanged between the lagoon and the open sea through three inlets (500-1000 m wide and from  
76 8 to 17 m deep) and it propagates to the city centre along a complex pattern of very shallow areas and canals (from 2 to  
77 20 m deep). The lagoon is separated from the sea by two long (about 25 km in total) narrow (less than 200 m average  
78 width) sandy barrier islands, reinforced with artificial defences in the most vulnerable parts. The elevation of these islands

---

<sup>1</sup> <https://repository.tudelft.nl/islandora/object/uuid:ea34a719-79c1-4c6e-b886-e0d92407bc9d?collection=education>

79 is such that they are not submerged during the most extreme events, with the exception of the 4<sup>th</sup> November 1966 flood,  
80 when they were breached at several points.

81 A clear relationship exists between the frequency of floods and RSL rise, resulting from the superposition of vertical land  
82 motion (at multiple space and time scale) and mean sea level (MSL) rise, which is projected to greatly increase flood  
83 risks in the future (e.g. Lionello et al. 2021). The RSL rise issue is extensively discussed in a complementary review  
84 article in this special issue (Zanchettin et al., 2021), to which the interested reader is addressed for detailed information.

85 However, ~~RSL rise this~~ is not the only factor playing a role in flooding. Section 2.1 provides a general framework for the  
86 identification of the different ~~contributors to RSL anomalies. They include a diversity of~~ factors acting at different time  
87 scales. ~~Extreme water levels~~Floods are caused by weekly to hourly atmospheric forcing, ~~and~~ affected by long-term  
88 (seasonal to decadal) ~~sea level~~ variability, ~~which in turn depends on~~ and intensified by the long-term (multidecadal to  
89 centennial) RSL ~~trends~~ rise (section 2.1). The timing of the surges produced by the atmospheric forcing with respect to  
90 the phase of astronomical tide and free oscillations (seiches) can substantially affect ~~the actual maximum~~ floods ~~sea level~~  
91 (sections 2.1 and 2.2). In fact, the length of the basin (Fig. 1) and the average speed of barotropic shallow water waves  
92 combine in such a way that the period of the free oscillations is close to the diurnal and semidiurnal components.  
93 Therefore, the basin is close to resonant conditions and the North Adriatic has ~~the largest tides in the Mediterranean Sea~~  
94 ~~(an astronomical tidal range more of about than~~ 1 m at the northern end of the basin, which is relevant for ~~extreme sea~~  
95 ~~levels in the floods of~~ Venice (Figure 1). The combination of all these forcings largely explains the historical floods, which  
96 are to some extent heterogeneous in terms of the leading factors (see section 2.2 and appendix A1).

97 ~~Storm surges, which are particularly important because they~~ often ~~yield~~ produce the largest contribution to ~~extreme sea~~  
98 ~~level~~ the floods, ~~and in the Adriatic Sea they~~ are caused by cyclones (~~as described in~~ see section 3.1). An important  
99 characteristic of the Adriatic Sea (particularly its northern area) is its proximity to the main cyclogenesis area of the  
100 western Mediterranean Sea, where cyclones initiate their south-eastward propagation along the Mediterranean storm track  
101 and (in a small number of cases) towards central Europe (e.g., ~~(~~Lionello *et al.*, 2016). In autumn and winter, the area  
102 around the Adriatic Sea is frequently crossed by these cyclones. The resulting south-easterly wind (Sirocco) when  
103 channelled along the main axis of the basin by the action of the Apennines and Dinaric Alps is essential for producing  
104 the storm surge ~~contribution to the extreme sea levels~~ in the northern Adriatic Sea and floods of Venice. At longer time  
105 scales, the frequency and/or severity of extreme water heights ~~Extreme sea levels~~ have also been associated with large-  
106 scale atmospheric variability and astronomical (solar) forcing. Available evidence of these links and their dynamics is  
107 reviewed in sections 3.2 and 3.3.

108 A major concern is the future evolution of ~~sea level extremes~~ floods. Section 4 is devoted to past and future changes in  
109 the frequency and magnitude of ~~sea level~~ extremes, and the relative roles of RSL rise and atmospheric forcing at different  
110 time scales. Section 4 also considers the most recent estimates of the future extremes ~~sea levels~~ and their dependence  
111 on the climate scenarios. The last section 5 provides a general assessment of the existing knowledge ~~and as well as~~  
112 indications of major gaps and needs for future research.

113 **2. Dynamics and characteristics of ~~sea level evolution during an~~ extreme floods**  
114 Extreme floods of Venice are caused by extremes or high-end values of the local instantaneous thickness of the ocean,  
115 hereafter called water height. The water height is defined as the difference between the instantaneous sea level and a local  
116 reference level, both measured with respect to a fixed reference level (which could be the reference ellipsoid, the geoid,

117 or a geocentric reference frame). In Venice, the local reference level moves vertically, because of land subsidence. The  
118 water height and the total thickness of the water column differ by a constant value, which is the depth of the sea bottom  
119 with respect to the local reference level (Fig. 2). Water height extremes and sea level extremes differ because the latter  
120 do not consider the effect of subsidence, which is important in Venice. Water height extremes result from contributions  
121 with different time scales and characteristics that are described in the next subsection.

#### 122 1.1.2.1. Tides, seiches and atmospherically forced sea level anomalies

124 This section describes the factors that contribute to ~~sea level water height fluctuations anomalies~~ in the North Adriatic  
125 Sea: astronomical tides, seiches, ~~and~~ atmospherically forced fluctuations, ~~(which include consist of~~ meteotsunamis, storm  
126 surges and surges caused by planetary atmospheric waves (PAW), ~~interdecadal to seasonal (IDAS) and relative~~ sea level  
127 ~~variations rise (RSLR) and RSL rise~~. These factors ~~are~~ are characterized by different dynamics and time scales. In general,  
128 they do not have the same importance in terms of contribution to extreme ~~sea level events~~ water heights, which have  
129 mostly been attributed to large storm surges, whose effect ~~was can be~~ reinforced or attenuated by the remaining factors.  
130 The classification of the atmospherically forced fluctuations in three categories is based on the scale of the meteorological  
131 forcing process: mesoscale ~~for meteotsunamis (tens of kilometres, minutes to hours)~~, synoptic scale ~~for storm surges~~  
132 ~~(thousands of kilometres, days)~~ and planetary scale ~~(tens of thousands of kilometres, weeks to months) for PAW surges~~  
133 ~~(see section 2.2)~~. At longer time scales, inter-decadal, inter-annual and seasonal (IDAS) sea level variability ~~and local~~  
134 ~~RSL rise, natural and human induced land subsidence, and sea level rise (SLR)~~ also contribute to ~~sea level water height~~  
135 extremes. Local RSL rise is the increase of local sea level relative to the local solid earth surface (Fig. 2 and Gregory et  
136 al., 2019) and it can be directly estimated by averaging local tide gauge data over a conveniently long period. It is caused  
137 by vertical land movements and changes of local MSL. The evolution of the RSL and IDAS in Venice, and of their  
138 different contributions is described in Zanchettin et al. (2021) in this special issue. The addition of storm surges,  
139 meteotsunamis and PAW surges represents the meteorological surge contribution to the water-height anomalies. The  
140 combined effect of seiches, astronomical tides and meteorological surge is generically referred to as detrended water  
141 height in this manuscript (Fig. 2), meaning that variability at seasonal and longer time scale is subtracted.

142  
143 Astronomical tides in the Adriatic Sea have a mixed semidiurnal cycle with two high and two low tide levels of different  
144 height every day. There are 7 components with amplitude above 1 cm and only 3 above 10 cm, with the semidiurnal  $M_2$   
145 and  $S_2$ , and diurnal  $K_1$  tides providing the largest contributions. The values of  $M_2$ ,  $S_2$  and  $K_1$  are approximately 23, 14,  
146 16 cm both outside the lagoon and in the Venice city centre. Tides consist of two Kelvin waves oppositely travelling  
147 along the basin at semidiurnal periods (Hendershott and Speranza, 1971) and of topographic waves travelling across the  
148 basin at diurnal periods (Malačić, ~~Viezzoli and Cushman-Roisin et al.~~, 2000). They are adequately reproduced by a  
149 number of numerical models (e.g. Janeković and Kuzmić, 2005; Lionello, ~~Mufato and Tomasin et al.~~, 2005; Ferrarin,  
150 ~~Maieu and Umgiesser et al.~~, 2017). Both diurnal and semidiurnal components have their maximum amplitude at the  
151 northern shore of the basin, in association to antinodes of seiches (see below). The semidiurnal components have an  
152 amphidromic point in the centre of the Adriatic (Franco *et al.*, 1982).

153 Seiches in the Adriatic ~~are standing waves with a node at the southern boundary of the basin and an antinode at the~~  
154 ~~northern shore. The periods of the basic modes are estimated at about 21.3 h and 10.8 h (Manca, Mosetti and Zennaro,~~  
155 ~~1974) and their patterns mimic those of the diurnal and semidiurnal tides, respectively. Seiches are commonly produced~~

156 after a surge, when the wind drops or switches from Sirocco (south-easterly) to Bora (north-easterly) and the water  
157 accumulation in the north Adriatic ceases to be supported by the wind stress. The Adriatic seiches are damped relatively  
158 slowly, with the decay time of fundamental mode amounting to 3.2 days (Cerovečki, Orlić and Hendershott, 1997), due  
159 to a weak frictional dissipation inside the basin and a small energy loss to the Mediterranean Sea. There is a long tradition  
160 of numerical modelling of the Adriatic seiches (e.g. Lionello, Mufato and Tomasin, 2005), but more accurate predictions  
161 of their periods and decay are still needed, e.g., (Bajo *et al.*, 2019).

162 **Storm surges** in the Adriatic have been extensively studied due to the need to forecast the floods of Venice (Robinson,  
163 Tomasin and Artegiani *et al.*, 1973), see Umgiesser *et al.*, 2020-2021 in this issue for a review). ~~The response of the sea~~  
164 ~~to air pressure forcing is close to the inverted barometer effect at daily time scales, e.g., (Karabeg and Orlić, 1982).~~  
165 However, the storm surge magnitude at the Venetian coast is mostly determined by the wind blowing over the shallow  
166 water areas over the North Adriatic Sea, ~~whose~~ The wind contribution to sea level along the Northern at the coast is  
167 typically 10 times larger than the inverse barometer effect (Bargagli *et al.*, 2002; Conte and Lionello, 2013; Lionello,  
168 Conte and Reale, *et al.*, 2019). Storm surges are produced by two main ~~winds~~ wind configurations: Sirocco blowing over  
169 the whole basin and a combination of Bora over the north Adriatic and Sirocco over the south Adriatic (Fig. 1). Depending  
170 on the structure of the wind field, flooding is more pronounced along the west or the east Adriatic coast (Međugorac *et*  
171 *al.*, 2018).

172 Seiches in the Adriatic are standing waves with a node at the southern boundary of the basin and an antinode at the  
173 northern shore. The periods of the basic modes are estimated at about 21.3 h and 10.8 h (Manca *et al.*, 1974) and their  
174 patterns mimic those of the diurnal and semidiurnal tides, respectively. Seiches are commonly produced after a storm  
175 surge, when the wind drops or switches from Sirocco (south-easterly) to Bora (north-easterly) and the water accumulation  
176 in the north Adriatic ceases to be supported by the wind stress. The Adriatic seiches are slowly damped with the decay  
177 time of fundamental mode amounting to 3.2 days (Cerovečki *et al.*, 1997), due to a weak frictional dissipation inside the  
178 basin and a small energy loss to the Mediterranean Sea. There is a long tradition of numerical modelling of the Adriatic  
179 seiches (e.g. Lionello *et al.*, 2005), but more accurate predictions of their periods and decay are still needed, e.g., (Bajo  
180 *et al.*, 2019).

181 **Meteotsunamis** are meteorologically-generated long ocean waves in the tsunami frequency band (Vilibić and Šepić, 2009;  
182 Šepić *et al.*, Vilibić and Belušić, 2009). They are generated by mesoscale air-tmospheric pressure disturbances that  
183 resonantly generate a traveling sea level anomaly, when their speeds of propagation approach that of the shallow-water  
184 barotropic waves. Adriatic mMeteotsunamis pose a major hazard on the eastern Adriatic coast, where their resonant  
185 periods are close to those of the normal modes of the bays/harbors.

186 **Long planetary atmospheric waves** propagate slowly and with wavelengths ranging from 6000 to 8000 km. They produce  
187 a long-term meteorological forcing and eventually long-lasting sea level anomalies (**PAW surges**), which establish  
188 favourable day-lastingbackground conditions for flooding (Pasarić and Orlić, 2001).

189 ~~The combination of storm surge, meteotsunamis and PAW surge represents the direct action of the meteorological forcing~~  
190 ~~on extreme sea levels and it is collectively termed **surge** in this manuscript, when no distinction is possible among the~~  
191 ~~different contributions.~~

192 The factors considered so far allow an interpretation of a typical flood (“aqua alta”, e.g. Robinson *et al.*, 1973). When a  
193 cyclone moves from western Mediterranean towards the Adriatic, low air-atmospheric pressure and Sirocco wind support

194 an increase of sea level/water height in the northern Adriatic Sea and potential flooding of the area. When the cyclone  
195 leaves the Adriatic area, air-atmospheric pressure increases while the Sirocco slackens or changes to Bora. Consequently,  
196 sea level decreases and seiches may be generated. Therefore, in the Adriatic storm surges and seiches represent two  
197 distinct phases of the response to the atmospheric forcing, one in which sea level rises under direct atmospheric forcing,  
198 and the other in which sea level relaxes – possibly through a series of damped oscillations. If a successive storm surge  
199 develops before the attenuation of the seiches induced by a previous event, a constructive or destructive superposition  
200 may occur (Bajo *et al.*, 2019). Analogously, the phase of tide during the period when the storm surge is large, can  
201 substantially increase or decrease the actual sea level maximum.

202 The contribution of meteotsunamis and PAW surges to extreme sea-level events in Venice has not been thoroughly  
203 investigated to date. However, the recent 12 November 2019 event uncovered their important role in flooding in Venice  
204 (Ferrarin *et al.*, 2021). Therefore, in general, the hazard and probability of an extreme sea level should also include these  
205 two contributions (see section 2.2).

206 Water-height values are This is further modulated by IDAS sea-level variability (caused by changes in marine circulation,  
207 characteristics of the water masses and by the action of teleconnection patterns) and RSL changes. *RSL changes*  
208 represents a long-term process (see Zanchettin *et al.* 2020, in this special issue, for a comprehensive review of its past and  
209 future evolution). *It and RSL rise* has been the dominant factor responsible for the significant increase of frequency of  
210 floods of the Venice city centre (Lionello *et al.*, 2012b).- In the last century, it has been caused almost equally by the  
211 increase of the mean level of the sea surface and the decrease of the land level because of natural and anthropogenic  
212 subsidence (see Zanchettin *et al.* 2021, in this special issue, for a comprehensive review of its past and future evolution).

213 The floods of Venice do not occur because water overtops coastal barriers or defences. In fact, the elevation of the natural  
214 barriers separating the lagoon from the Adriatic Sea has so far prevented wave overtopping, with the unique exception  
215 (already mentioned in the introduction) of the 1966 flood, when waves may have contributed to increase water height in  
216 the lagoon. Therefore, wave run-up and infra-gravity waves and nearshore processes (though certainly relevant along the  
217 sea-side front of the barrier islands under some conditions) have never been considered when computing water-height  
218 extremes inside the lagoon. It cannot be excluded that these factors will become relevant under extreme sea level rise in  
219 the future, but present evidence is that waves do not need to be considered for computing the water height in the Venice  
220 city centre (Roland *et al.*, 2009), as long as barrier islands continue being protected by coastal defences and maintained  
221 by beach nourishment.

222 It is well known that tidal and non-tidal components have a certain degree of interaction in shallow water areas with large  
223 tidal excursions where non-linear effects are significant (e.g Horsburgh and Wilson, 2007, and references therein).  
224 However, in a recent global scale investigation on the non-linear interactions between the tide and non-tidal residuals  
225 (Arns *et al.*, 2020) only a small negative effect on extreme sea levels in the northern Adriatic Sea has been found. In fact,  
226 in the northern Adriatic Sea, given the relatively small importance of tidal excursions (about 1 m) compared to the local  
227 water depth (average depth of about 35 m), it is reasonable to neglect the effect of tides on the storm surge propagation.  
228 Such assumption is confirmed by a long past prediction practice with hydrodynamic models, where only the  
229 meteorological forcing was used and the astronomical tide was either added to the model results to get the actual  
230 prediction or subtracted to the observations for model validation. Examples of this approach and of its success are Lionello  
231 *et al.* (2006), Bajo *et al.* (2007), Mel and Lionello (2014) among many others. Such an assumption has been confirmed  
232 by several high-resolution numerical studies demonstrating that tide-meteorological surge interactions are small, even

during the most severe events (Roland et al., 2009; Cavaleri et al., 2019). An example of such simulations can be found in Appendix B and it shows that nonlinear interactions are lower than 5% at the peak of the water height.

### 1.2.2.2. A description of the largest past events

Regular ~~instrumental tide gauge~~ observations in Venice started in 1871. Since 1919 ~~sea level value~~ observations have been ~~referenced~~ to their mean ~~sea level level~~ over the 1884-1909 period (central year 1897), which is ~~the local reference level used for water-height values and is~~ usually called ‘Zero Mareografico Punta Salute’ (ZMPS), ~~and referred to as relative sea level (RSL)~~. The history of Venice tide gauges, their reference planes and the related geodetic connections ~~were have been~~ described and discussed by Dorigo, (1961a.) ~~and (Battistin and Canestrelli, 2006)~~. (Battistin and Canestrelli (2006) reviewed the observations from 1872 to 2004 and provided a complete list of ~~daily maxima and minima high and low sea level data~~ with the relevant primary data sources. ~~Sea level Tide gauge~~ data are also available in the web sites of ~~the~~ Istituto Superiore per la Protezione e la Ricerca Ambientale (ISPRA), Servizio Laguna di Venezia ([www.venezia.isprambiente.it](http://www.venezia.isprambiente.it)), and ~~the~~ Centro Previsione e Segnalazione Maree of ~~the~~ Venice municipality ([www.comune.venezia.it/content/centro-previsione-e-segnalazione.maree](http://www.comune.venezia.it/content/centro-previsione-e-segnalazione.maree)).

The Venice Municipality defines ~~a high large RSL~~ events (‘acqua alta’) when ~~relative sea level (RSL) the water height~~ exceeds 80 cm ~~(above ZMPS)~~, ~~a severe and exceptional~~ events when it exceeds 110 cm and ~~an exceptional event when it exceeds~~ 140 cm, ~~respectively~~. Since 1872, ~~there have been 140 cm threshold has been exceeded during~~ 18 ~~exceptional~~ events. Depending on the phase of the astronomical tide and of other factors, ~~very high RSL large water heights~~ can or cannot correspond to very high storm surges. Table 1 list the ~~highest RSL largest water heights events~~<sup>2</sup> alongside the contributions of various factors (in a similar way as previously done by (Orlić, 2001):

~~RELATIVE EXTREME SEA LEVEL WATER HEIGHT =~~ STORM SURGE + PAW SURGE + METEOTSUNAMI ~~and MAV setup~~ + ASTRONOMICAL TIDE + SEICHE + IDAS ~~Variability~~ ~~ARIABILITY~~ + RSLR

~~In order to~~ ~~For computing compute~~ the values in ~~T~~table 1, the long-term ~~water level~~ time series of Punta della Salute was processed with a tidal harmonic analysis tool based on the least squares fitting (Codiga, 2011) to separate the tidal from the other contributions ~~to the total sea level~~. The residuals ~~sea levels~~ were detrended ~~for RSLR~~ using a 10-year centered running mean ~~to determine the RSL rise~~.

~~The other~~ contributions ~~of~~ (storm surge, PAW surge, ~~meteotsunami~~ ~~meteotsunamis~~ and mesoscale atmospheric variability (MAV), ~~local setup~~, seiches, IDAS variability) ~~were have been~~ estimated using ~~band-pass~~ digital filters (~~low pass, band pass and high pass, as described in Ferrarin et al., 2020~~) in the time domain assuming Fourier decomposition, ~~following Ferrarin et al., 2021~~. ~~The procedure is straightforward for seiches and tides, which can be isolated by applying band-pass filters around their known frequencies. The criteria are more complicated when considering the response of sea level to the atmospheric forcing because it is characterized by a continuous spectrum. A general distinction by Holton (2004), based on the different space-time scales of the atmospheric phenomena, considers planetary-scale (order of 10<sup>7</sup> m), synoptic-scale (order of 10<sup>5</sup>-10<sup>6</sup> m) and mesoscale motions (order of 10<sup>4</sup>-10<sup>5</sup> m). At the planetary scale Rossby waves move westwards against the eastward zonal flow and are therefore characterized by relatively small speeds (1–10 m/s) and long time scales (from 10 days to 100 days). Synoptic-scale systems (mostly driven by baroclinic instability) tend to~~

<sup>2</sup> Some significant surges may have been missed before 1933 due to lack of information, while all the high RSL events are available since 1872.

269 move eastwards with the mean flow and are marked by relatively large speeds (typically 10 m/s) and time scales of about  
270 a few days. Mesoscale systems (which are topographically forced or are driven by instabilities operating at that scale)  
271 have also relatively large speeds, of the order of 10 m/s (Markowsky and Richardson, 2010) and characteristic time scales  
272 in the range from 10 minutes to few hours. A 10-day period for the separation between planetary and synoptic scales is  
273 supported by the cross-spectral analysis of the 500 hPa geopotential height and sea level for the Adriatic (Orlić, 1983),  
274 which show indeed high (low) coherence above (below) this threshold. A 10-hour cut-off period allows to distinguish  
275 between synoptic-scale and MAV setup (including Meteotsunamis), as the latter has time scales in the range from the 10-  
276 min period of a pure buoyancy oscillation to the 17-hour period of mid-latitude inertial oscillations (Markowsky and  
277 Richardson, 2010). On a practical basis, Ferrarin *et al.* (2021) have used the 10-hour threshold for separating responses  
278 to a cyclone moving in an eastward direction above the Mediterranean from a low-pressure meso-scale system travelling  
279 in a northwestward direction along the west Adriatic coast in their analysis of the 12 November 2019 even. The value  
280 separating storm surge and PAW surge was set to 10 days and that the corresponding value for storm surge and  
281 meteotsunami (including also local set up in the lagoon) was set to 10 hours. The separation between ~~the~~ PAW surges  
282 and IDAS variability was achieved by applying a low pass filter with the cut-off period placed at 120 days. The values of  
283 the contributions to water heights above 140 cm are shown in Table 1. Overall, the ~~events listed in Table 1~~ agrees with  
284 the ones compiled in other studies since the beginning of instrumental observations (Dorigo, 1961b; Livio, 1968;  
285 Canestrelli *et al.*, 2001). The frequency of water heights follows a strong seasonal cycle (Lionello *et al.*, 2012b). The most  
286 intense events (with maxima above the 99th percentile) occur in November and December, with November concentrating  
287 the largest number of intense events. However, severe events (maxima above the 80th percentile) can occur from late  
288 September to early May and, very rarely also in summer.

289 The event of 4 November 1966 corresponds to both the ~~highest~~ highest storm surge and the ~~highest RSL~~ largest water  
290 height ever recorded in Venice. Other outstanding events are those observed on 22 December 1979 and 12 November  
291 2019. The event of 29 October 2018 consists of two peaks ~~that occurred separated by 6 hours apart,~~ with similar ~~RSL~~  
292 water-height values (148 and 156 cm), but quite different phases of the astronomical tide, so that the higher water level  
293 corresponds to the lower storm surge. This is the only example in 147 years of two such high ~~RSL~~ water level peaks in  
294 such a short time interval. November 2019 is also peculiar because four ~~RSL~~ water-height peaks with at least 140 cm  
295 height occurred on 12, 13, 15 and 17. The event of 12 November 2019 was particularly severe, reaching 189 cm ~~RSL~~.  
296 This was the second highest ~~ever recorded~~ ever-recorded RSL water height. In this case the storm surge was relatively  
297 modest, and the exceptional water level was caused by the superposition of PAW surges, positive astronomical tide and  
298 an unprecedented contribution caused by a meteotsunami. After the exceptionally high water on 12 November, three  
299 successive events with water height above 140 cm occurred in just five days. As reported in Ferrarin *et al.* (2021), these  
300 events were driven by three separate Sirocco wind episodes in the Adriatic Sea, which did not trigger any significant  
301 seiche. These flood events were determined by the overlapping of the maximum meteorological contribution, the tide  
302 peak and a persistent high monthly mean sea level in the northern Adriatic. It should be stressed that ff Four of the eight  
303 ~~highest RSL~~ largest water heights values since 1872 were observed during the autumn seasons of 2018 and 2019.

304 The ~~amplitude of the~~ astronomical tide ~~makes it~~ is an important contribution to the actual ~~sea level~~ water-height extremes  
305 and the time lag between the surge peak and the nearest astronomical tide maximum may make a substantial difference.  
306 Considering the events described in Appendix AI, if surge and tide had peaked together, the observed ~~RSL~~ water height,  
307 based on the linear superposition of the different factors (a reasonable first-order approximation for the Adriatic Sea)  
308 would have approximately been 220 cm, both on 4 November 1966 and 29 October 2018 (second peak), and 215 cm on



309 12 November 1951. Particularly, for the second peak of 29 October 2018 ~~the large negative contribution of the~~  
310 ~~astronomical tide played an essential role limiting the severity of the event~~~~the large magnitude of negative astronomical~~  
311 ~~tide contribution has an essential role to limit the impact of the event.~~ On the contrary, the coincidence of a moderate  
312 storm surge with a preexisting seiche and a high astronomical tide level produced the sixth highest ~~level~~water height in  
313 ~~Table 1~~the records. In conclusion, ~~the comparison among the different contributions in Table 1 shows that~~ storm surge  
314 represents often the largest contribution, but, in several cases, also other factors play a fundamental role. Particularly, in  
315 the case of 12 November 2019, ~~(the second highest ever-recorded~~ sea level~~water height)~~ several other factors exhibited  
316 contributions comparable to the storm surge~~has been produced by comparable contribution from several factors, with a~~  
317 ~~storm surge value, which was not particularly high~~whose value was rather moderate.

318 The meteorological and marine conditions that led to major storm surge events have been assessed with reanalyses and  
319 dedicated model simulations, including the catastrophic storm surges of 4 November 1966 (De Zolt *et al.*, 2006; Roland  
320 *et al.*, 2009; Cavaleri *et al.*, 2010), 22 December 1979 (Cavaleri *et al.*, 2010), 1 December 2008 (Medugorac *et al.*, Pasarié  
321 and Orlié, 2016), 1 November 2012 (Medugorac *et al.*, Pasarié and Orlié, 2016), 12 November 2019 (Ferrarin *et al.*, 2021)  
322 (ISPRA and CNR-ISMAR, 2020). Bertotti *et al.* (2011) modelled five important events that occurred between 1966 and  
323 2008. Appendix AI ~~includes the descriptions~~describes the largest of major surge and RSL ~~water height~~ events and related  
324 meteorological situations.

325 ~~The frequency of storm surges follows a strong seasonal cycle (Lionello *et al.*, 2012b). The most intense events (with~~  
326 ~~maxima above the 99th percentile) occur in November and December, with November concentrating the largest number~~  
327 ~~of intense events. However, severe events (maxima above the 80th percentile) can occur from late September to early~~  
328 ~~May, and, very rarely also in summer.~~

### 329 1.4.2.3. **The propagation of the sea-level signal in the interior of the lagoon**

330 North Adriatic sea level~~water height~~ anomalies first propagate into the lagoon through the three inlets, and then follow  
331 the tidal channels (Fig. 1, right panel). The major channels inside the lagoon are up to 10 meters deep, and this results in  
332 a propagation speed of about 10 m/s (Umgiesser *et al.*, 2004). The water then expands laterally into the shallow flats,  
333 where propagation of the wave is much slower.

334 Astronomical tides in the southern and central basins of the lagoon are slightly amplified with respect to the inlets, because  
335 of resonance effects between the tide (both diurnal and semidiurnal) and the size of the basin. In the northern part of the  
336 lagoon, characterized by mud flats, islands and salt marshes, dissipative processes dominate over the resonance condition,  
337 so that the tidal wave shows an attenuation of about 50 % of the incoming tide (Ferrarin *et al.*, 2015). As a consequence  
338 of natural and anthropogenic morphological changes that occurred in the lagoon in the last century, the amplitude of  
339 major diurnal and semi-diurnal tidal constituents grew significantly, with a consequent increase in extreme high sea levels  
340 in Venice (Ferrarin *et al.*, 2015).

341 The surge signal, once it has entered ~~inside~~ the lagoon, ~~is able to~~ propagates nearly without damping to the city  
342 center~~centre~~, where sea-water levels are comparable to the ones close to the inlets with a typical 1 hour delay (Umgiesser  
343 *et al.*, 2004). Other more remote areas of the lagoon show a higher phase shift with respect to the inlets of up to 3 hours.  
344 With strong NE (Bora) or SE (Sirocco) winds, the difference between water levels in the south and the north side of the  
345 lagoon may exceed 50 cm (Mel *et al.*, 2019). The Venice city centre is relatively little affected by these differences, since

346 it is close to the node of the oscillations. However, the strong setup at the southern part of the lagoon can lead to flooding  
347 in the city of Chioggia.

348 Figure 3 shows the amplification factor (percentage, values higher/lower than 100 correspond to  
349 amplification/attenuation) of sea level oscillations in the Venice city centre with respect to their amplitude at the lagoon  
350 inlets as a function of their period. This computation is based on the model of Umgiesser *et al.* (2004). In the present  
351 situation long period oscillations ( $\geq 24$  hours) at the inlets propagate undisturbed into the lagoon, short ones ( $\leq 3$  hours) are  
352 very effectively damped and at intermediate periods they reach an amplification maximum of about 120% at 9 hours.  
353 Numerical experiments with the same model and no frictions suggest that this effect is caused by the combination of  
354 internal resonances occurring in the range from 10 to 5 hours with the strong friction inside the shallow lagoon. In the  
355 hypothetical case with very shallow inlets (maximum depth equal to 6 m) all periods below 12 hours are heavily damped.  
356 This shows that lowering the depth of the inlets would lower the water-height maxima inside the lagoon, though with  
357 problematic consequences in terms of reduced shipping, water exchange and strong erosion inside the inlets. A 1 m RSL  
358 rise (without any change in the morphology of the lagoon) would amplify the lagoon response, showing the possibility of  
359 higher extremes in the future.

360 ~~With strong NE (Bora) or SE (Sirocco) winds, the difference between sea levels in the south and the north side of the~~  
361 ~~lagoon may exceed 50 cm (Mel, Carniello and D'Alpaos, 2019). The Venice city center is relatively little affected by~~  
362 ~~these differences, since it is close to the node of the oscillation of the water level. However, the strong setup at the southern~~  
363 ~~part of the lagoon can lead to flooding in the city of Chioggia.~~

364

## 365 2.3. Atmospheric patterns associated with extreme storm surges

### 366 2.1.3.1. Characteristics of cyclones producing storm surges and floods of Venice

367 The Mediterranean region is characterized by a high frequency of cyclone ~~one of the areas in the Northern Hemisphere~~  
368 ~~where cyclone activity is more frequent~~ due to a wide range of factors and mechanisms that acting in the region which  
369 ~~favour several~~ cyclogenesis ~~processes~~ (Trigo *et al.*, ~~Davies and Bigg~~, 1999; Lionello *et al.*, 2006a; Ulbrich *et al.*,  
370 ~~Leekebusch and Pinto~~, 2009; Lionello *et al.*, 2012a; Ulbrich *et al.*, 2012; Lionello *et al.*, 2016). These systems are often  
371 associated with extreme weather events (Jansa *et al.*, 2001; Lionello *et al.*, 2006a; Toreti *et al.*, 2010; Ulbrich *et al.*, 2012;  
372 Reale and Lionello, 2013) ~~and, more specifically, with large~~ storm surges along the Mediterranean coastline and floods  
373 of Venice (Canestrelli *et al.*, 2001; Trigo and Davies, 2002; De Zolt *et al.*, 2006; Lionello *et al.*, 2012b; Lionello *et al.*,  
374 ~~Conte and Reale~~, 2019). Cyclones produce storm surges by two mechanisms: the inverse barometric ~~effects~~ effects caused  
375 ~~by (resulting from~~ the decrease of atmospheric pressure during their ~~eyelone~~ transit over the area), and the wind set-up  
376 ~~(caused by the intense eyelonic air flows surface wind, typically Sirocco, channelled by the topography along the main~~  
377 ~~axis of the Adriatic Sea, which that~~ piles up water masses against the coast of the Northern Adriatic (Lionello *et al.*, ~~Conte~~  
378 ~~and Reale~~, 2019).

379 Figure ~~2-4~~ shows the temporal evolution of mean sea-level pressure (MSLP) and 10 meter wind fields during intense  
380 storm surge events. It is a composite based on the floods with a storm surge contribution higher than 50 cm ~~in Venice~~ in  
381 the period 1979-2019 (Table 1) using ~~the hourly MSLP fields of~~ ERA5 reanalysis (Hersbach *et al.*, 2020). The time lags  
382 chosen for the composites ~~is are~~ 36, 24-, 12 hours before and 12, 24 hours after the peak of the events ~~(reported in Table~~  
383 ~~1). Figure 3-5 shows the same information, though it is based on the remaining events in T~~ table 1, when (with a the storm

384 surge contribution lower ~~component did not exceed~~ than 50cm). In both figures ~~at the peak of the event,~~ the pressure  
385 minimum is located in the Gulf of Genoa ~~at the peak of the event,~~ but in ~~Figure 42~~ the cyclone is deeper and the MSLP  
386 gradient along the Adriatic Sea is larger. ~~These differences have strong impacts on the intensity of the wind fields, their~~  
387 ~~spatial structure and direction in the Adriatic Sea (small panels in Figs. 4 and 5), modulating the part of the Adriatic~~  
388 ~~coastline that is most affected by the storm surge (Medugorac et al., 2018). Indeed, the first predictions of floods in Venice~~  
389 ~~were based on an autoregressive model considering as inputs the MSLP cross-basin differences (Tomasin and Frassetto,~~  
390 ~~1979).~~ Further, the evolution of the cyclone before and after the ~~water~~ peak of the ~~sea-level-anomaly~~ storm surge is  
391 different ~~in Figs. 4 and 5~~. In ~~Figure 2-4~~ cyclogenesis occurs ~~close to the Iberian coast~~ in the western Mediterranean Sea  
392 (as noted in ~~(Lionello et al., 2012b)~~, ~~close to the Iberian coast, as with~~ a MSLP minimum well separated from the  
393 background field. In ~~Figure 3-5~~ cyclogenesis occurs in the ~~northwestern~~ north-western Mediterranean Sea within the  
394 flow produced by a ~~preexisting~~ pre-existing cyclone, whose ~~center~~ centre is located north of the Alps. In both ~~figures~~  
395 ~~composites~~ the lee cyclogenesis processes and the generation of a secondary minimum is evident (Trigo and Davies,  
396 2002; Lionello, 2005; Lionello et al., 2012b; Lionello et al., Conte and Reale, 2019) and the pressure gradient along the  
397 Adriatic Sea intensifies and becomes almost parallel to the basin coastlines. This synoptic configuration produces a  
398 decrease of the atmospheric pressure above ~~n~~ Northern Italy and an increase of intensity of ~~the~~ atmospheric flow in the  
399 Adriatic Sea directed towards its northern coast, which results in the increase of sea level in Venice, e.g. (Lionello et al.,  
400 1998).

401 Figure ~~4-6~~ shows the density (contours) of tracks of cyclones (measured ~~as % in percentage~~ relative ~~to the total~~ frequency  
402 of cyclones in each cell of 1.5° ~~degree~~) producing ~~relative-sea-level~~ a water height higher than 110 cm  
403 (<https://www.comune.venezia.it/it/content/grafici-e-statistiche>) in the period 1979-2019. ~~The figures~~ Figure 6 also reports  
404 ~~also~~ the tracks of ~~all the~~ cyclones ~~associated to all events~~ that are listed in ~~T~~ table 1 (cyan colour), ~~with the events of 4~~  
405 ~~November 1966, 29 October 2018 (Vaia storm) and 12 November 2019 in blue, red and green lines, respectively.~~ ~~of~~  
406 ~~November 4th 1966 (blu line), the Vaia storm 29 October 2018 (red line) and of 12 November 2019 (green line).~~ Cyclone  
407 tracks shown in ~~Figure Fig. 64~~ have been identified with an automatic detection and tracking scheme (Lionello et al.,  
408 ~~Dalan and Elvini, 2002)~~ applied to the ERA-5 MSLP fields ~~at a spatial resolution of 0.25° and a temporal resolution of 6~~  
409 ~~hours. The tracking scheme partitions the MSLP fields in depressions, which can be considered candidates for~~  
410 ~~independent cyclones, by merging all steepest descent paths leading to the same pressure minimum. Shallow secondary~~  
411 ~~minima with a small area are absorbed in the large nearest system, whose trajectory is computed by associating the~~  
412 ~~location of the low-pressure centres in successive maps within a minimum distance criterion until the system disappears~~  
413 ~~(cyclolysis). In that way, the method detects the formation of cyclones inside the Mediterranean and, at the same time,~~  
414 ~~avoids the inflation in the number of cyclones that would result from considering small, short-lived features as~~  
415 ~~independent systems. This method has been extensively described in previous works (Lionello, Dalan et al. 2002, Reale~~  
416 ~~and Lionello 2013, Lionello et al. 2016) and already used in numerous studies assessing the climatology of Mediterranean~~  
417 ~~cyclones, such as Lionello et al., (2016) and Flaounas et al., (2018), in the IMILAST tracking scheme intercomparison~~  
418 ~~analysis (Neu et al., 2013) and in a dedicated study on the synoptic patterns leading to high water levels along the coast~~  
419 ~~of the Mediterranean Sea (Lionello et al., 2019). Readers are addressed to those studies for details.~~

420 The density of tracks shown in ~~Figure Fig. 4-6~~ is characterized, ~~in the Atlantic sector,~~ by a ~~peculiar~~ north-west/south-east  
421 direction ~~in the Atlantic sector,~~ which is different from the usual south-west/north-east ~~direction-pattern of the regional~~  
422 ~~storm track observed in Atlantic~~ (Neu et al., 2013; Ulbrich et al., 2013; Reale et al., 2019). Moreover, ~~the density of track~~  
423 has a maximum in the ~~w~~ Western Mediterranean. As ~~also~~ shown in Lionello et al., 2012 the tracks of cyclones producing

424 the ~~strongest event-largest floods~~ (Table 1 and ~~FigureFig. 23~~) have distinctive characteristics with respect to the majority  
425 of cyclones crossing the Mediterranean Sea. ~~As shown in Figure 4 m~~Many of these systems enter the region from the  
426 ~~w~~West/~~S~~southw–West and follow a ~~N~~north–~~e~~Eastward direction. ~~On the other hand~~Differently, the majority of  
427 Mediterranean cyclones originate in the gulf of Genoa and follow a ~~s~~South–~~e~~East direction (Trigo ~~et al., Bigg and Davies,~~  
428 2002; Trigo ~~et al., Davies and Bigg,~~ 1999; Lionello *et al.*, 2006b; Ulbrich *et al.*, 2012; Lionello *et al.*, 2016). ~~In fact, the~~  
429 ~~position of the pressure minimum, the spatial structure of cyclone-induced wind fields over the Adriatic Sea and the~~  
430 ~~MSLP cross-basin differences largely affect the characteristics of the storm surge.~~ More recent studies ~~suggest-confirm~~  
431 that ~~a-the phase-lockingposition~~ of the cyclone with respect to the basin ~~seems to be~~is critical ~~to provide the optimal~~  
432 ~~conditions~~ for storm surges ~~in the north Adriatic-events, and its with small-variations in its position inducing induces~~ a  
433 veering of the onshore wind and even ~~opposite-negative~~ responses in sea level (Lionello ~~et al., Conte and Reale,~~ 2019).

434 The ~~diversity-peculiarity~~ of ~~triggering~~ cyclones ~~triggering storm surges~~ is also evidenced from a cluster analysis of the  
435 daily atmospheric fields associated ~~to with autumn surge events in Venice (Figure 5), the peaks above the 99.5th percentile~~  
436 ~~of the daily mean detrended water height obtained with a 6-month high pass filter (Fig. 7). Only peaks that are separated~~  
437 ~~by at least 3 days are considered to ensure the selection of independent extreme events. To ensure a large sampling size,~~  
438 ~~the analysis uses the NCEP/NCAR reanalysis data for the 1948-2018 period (Kalnay et al., 1996). A k-means clustering~~  
439 ~~(e.g. Wilks 2006) of the standardized anomalies of MSLP over the Euro-Atlantic sector and 10-m wind vectors over the~~  
440 ~~Mediterranean Sea has been applied to group events with similar spatial patterns. Clusters are constructed so that~~  
441 ~~differences between the daily patterns are minimized within the same cluster and maximized between the clusters, using~~  
442 ~~the sum of squared distances as metric. Each cluster is characterized by its centroid (the composited spatial pattern of~~  
443 ~~MSLP and 10-m wind standardized anomalies for all days in the cluster). The root mean squared difference (RMSD)~~  
444 ~~between the daily standardized fields of MSLP and 10-m wind vector of all considered events and their corresponding~~  
445 ~~centroid measures the total spread of the partition.~~ When all extremes ~~surges~~ are considered (Fig-ure 5a6a), the resulting  
446 ~~centroid~~ pattern resembles that of ~~FigureFigs.s 2-4 and 3-5~~ at the peak of the event, ~~since the majority of extreme surge~~  
447 ~~events occur in autumn (see next section).~~ However, the composite has a considerable spread (~~as measured by the root~~  
448 ~~mean squared difference~~large, RMSD), which can be reduced by progressively discriminating types of events (~~i.e.~~  
449 ~~increasing the number of clusters, with a k-means analysis (FigFig.- 65b)~~). Two clusters bring the steepest decrease in the  
450 RMSD distribution and capture the distinction between cyclones to the north and south of the Alps (~~FigFigs.- 75c,d~~)  
451 already reported by Lionello (2005).

452

### 453 2.2.3.2. Links to large scale patterns

454 Several studies have investigated links between the main modes of atmospheric circulation variability and ~~high~~  
455 ~~surgesfloods~~ in Venice (Fagherazzi *et al.*, 2005; Lionello, 2005; Zanchettin *et al.*, 2009; Barriopedro *et al.*, 2010;  
456 Martínez-Asensio ~~et al., Tsimplis and Calafat,~~ 2016). ~~The negative phase of the North Atlantic Oscillation (NAO) has~~  
457 ~~been associated with both high mean sea level and floods in Venice (Zanchettin et al., 2009), although this signal is absent~~  
458 ~~in autumn (when storm surges are larger). Indeed, the large-scale circulation pattern associated with Venice floods~~  
459 ~~(Lionello, 2005) is different to the NAO-, The North Atlantic Oscillation (NAO) has been found to exert no significant~~  
460 ~~influence on extreme surges, which are linked to a different large scale circulation pattern (Lionello, 2005),~~ being the  
461 East Atlantic (EA; (Martínez-Asensio *et al.*, 2014; Martínez-Asensio ~~et al., Tsimplis and Calafat,~~ 2016) or the East  
462 Atlantic-Western Russia (EAWR; (Fagherazzi *et al.*, 2005) the teleconnection patterns that exert the largest influence on  
463 their seasonal characteristics. ~~Another study found that the negative phase of the NAO is associated with both high mean~~

464 ~~sea level and floods in Venice (Zanchettin *et al.*, 2009), although this signal is absent in autumn (when surges are larger).~~  
465 Differences in the large-scale seasonal mean atmospheric circulation between active years (autumns with at least one ~~high~~  
466 ~~large meteorological surge~~<sup>3</sup>) and quiet years (autumns with no ~~high-large meteorological surge~~) have ~~also~~ been reported  
467 (Barriopedro *et al.*, 2010). The ~~favorable~~~~favoured~~ seasonal pattern for the occurrence of ~~large meteorological surges in~~  
468 ~~autumn surges~~ displays ~~little resemblance to the NAO, but a wave train with~~ a negative pressure ~~center~~~~centre~~ in central  
469 Europe, ~~similar to that found in the daily-based composite of Fig. 7~~~~abounded by two high pressure anomalies.~~

470 The aforementioned relationships are often weak, though, and hence potentially sensitive to metrics, thresholds and  
471 ~~analyzed~~~~analysed~~ periods. This blurred influence of teleconnection patterns is not surprising, taking into account that  
472 seasonally averaged indices do not necessarily capture short-term fluctuations, and that ~~favorable~~~~favoured~~ synoptic  
473 conditions (see ~~Fig.~~~~Fig.-~~ 57) might occur under different large-scale configurations. To avoid this, a Weather Regime  
474 (WR) approach is adopted herein, which predefines a number of recurrent large-scale atmospheric circulation patterns  
475 and assigns each day to one of them. Following (Garrido-Perez *et al.*, 2020), we considered eight WRs, which yields a  
476 fair representation of the variability all-year round. Almost half of the ~~extreme~~~~extreme event~~~~sea levels~~<sup>4</sup> in Venice are  
477 associated with the Atlantic Low (AL) WR (~~Figure~~~~Fig. 6a~~~~8a~~), whose canonical pattern (~~Figure~~~~Fig. 6b~~~~8b~~) strongly  
478 resembles that of Fig. 75d and of ~~Figure~~~~Fig. 8.6~~ of (Lionello 2005). The remaining cases (arguably many of the  
479 Mediterranean cyclones included in Fig. 75c) occur under different WRs without a clear preference, although some  
480 anticyclonic WRs (e.g. the Atlantic High) are ~~unfavorable~~~~unfavourable~~ for extreme ~~meteorological surges~~~~sea levels~~.  
481 Despite the strong association with AL on daily scales, ~~the Spearman's rank correlation r between the seasonal frequency~~  
482 ~~series of AL days and extreme events is low (r=0.26 for 1948-2018, p<0.05, where p is the significance level) and the~~  
483 ~~seasonal frequency series of AL days yields little skill on the corresponding occurrence of extreme surges (rho=0.26 for~~  
484 ~~1948-2018, p<0.05), which is~~ similar to that obtained from other less influential WRs (e.g. Zonal Regime, ~~rho~~~~=0.27;~~  
485 ~~p<0.05~~). This illustrates that the interannual variability of ~~detrended water-height~~ ~~seasonal~~~~extremes~~ ~~sea levels in autumn~~  
486 cannot be well described by fluctuations in the dominant patterns of atmospheric circulation variability over the Euro-  
487 Atlantic sector.

488

### 2.3.3.3. The role of solar cycles on extreme floods

489 Some studies have reported decadal fluctuations in the frequency of ~~extreme surges~~~~floods~~ in phase with the 11-yr solar  
490 cycle during the second half of the 20th century, such that periods of high solar activity have coincided with more frequent  
491 and persistent ~~extreme surges~~~~floods~~ in Venice (Tomasin, 2002; Lionello, 2005; Barriopedro *et al.*, 2010) and other  
492 Mediterranean coastal stations (Martínez-Asensio ~~et al.~~, ~~Tsimplis and Calafat~~, 2016). This signal results from the  
493 atmospheric forcing on sea level, as revealed by hindcasts of a barotropic ocean model forced with observed atmospheric  
494 pressure and winds (Martínez-Asensio ~~et al.~~, ~~Tsimplis and Calafat~~, 2016).

495  
496 An unanswered question is how such a small solar forcing ~~could~~ modulates the tropospheric circulation over the Euro-  
497 Atlantic sector. Several hypotheses have been proposed, including decadal variations of the regional atmospheric  
498 circulation that promote the constructive interference with the ~~favorable~~~~favoured~~ pattern for the occurrence of extreme  
499 ~~surges~~~~floods~~ during periods of high solar activity (Barriopedro *et al.*, 2010). Other studies claim for a solar modulation

---

<sup>3</sup> Events in which the meteorological surge exceeds the 95th percentile of the total distribution

<sup>4</sup> Events with ~~daily mean detrended water height~~~~maximum sea level~~ above the 99.5th percentile of the 1948-2018 distribution

500 of the stratospheric polar vortex and a lagged response of the NAO, e.g. (Thiéblemont *et al.*, 2015) and reference therein).  
501 However, this mechanism would mainly affect the winter NAO, rather than the decadal variability of autumn ~~extreme~~  
502 ~~floods~~~~surges~~ in Venice. In addition, modeling studies reveal negligible impacts of the 11-yr solar cycle on the NAO and  
503 demonstrate that decadal variations of the NAO can eventually vary in phase with the 11-yr solar cycle by random chance  
504 (Chiodo *et al.*, 2019). Given the lack of mechanistic understanding, the null hypothesis of internal variability cannot be  
505 rejected.

506 Indeed, an updated analysis of autumn extreme events (99.5th percentile) from the longest series of daily mean detrended  
507 water height RSL in Venice based on the data of (Raicich (2015), covering the period 1872-2018, shows that the 11-yr  
508 solar signal is no longer evident ~~in the frequency series of autumn extreme surges~~ since the ~2000s, nor it was present  
509 before the ~1950s (~~Figure Fig. 7-9~~ top panel). Significant correlations are limited to the period from 1970 to 2000  
510 (~~Figure Fig. 9~~, bottom panel) and give rise to strong co-variability during the second half of the 20th century, coinciding  
511 with the Grand Solar Maxima covered by most studies. Further, there is no indication of the presence of an 11-year  
512 periodicity in the ~~mean sea level series of autumn mean water height and its extremes (figure Figs. C1 in Appendix C III.1~~  
513 ~~and III.2)~~ and when extreme events are defined using different thresholds (Fig. C2 in Appendix C). These results suggest  
514 that if there is a solar signal it would likely be non-stationary (arguably masked by other sources variability) and/or non-  
515 linear (e.g. confined to Grand Maxima of solar activity). The alternative hypothesis is that the decadal variability of  
516 extreme surges is due to other causes, including internal variability. Therefore, either the solar signal is non-linear, non-  
517 stationary (arguably masked by other sources variability) or the decadal variability of extreme surges is due to other  
518 causes, likely internal variability. It is ~~reasonable~~ plausible that, superimposed on the uncontroversial increasing  
519 frequency of Venice flooding due to the ~~mean sea level RSL~~ rise, the frequency of extreme water heights will experience  
520 large interannual-to-decadal variations in the future, as it has been observed in the recent period. However, the causes of  
521 this variability are still uncertain~~large interannual to decadal variations will continue in the future, the causes of which~~  
522 ~~are still uncertain.~~

### 523 3.4. Past and future evolution

#### 524 3.1.4.1. Past evolution and recent trends of floods and extreme sea levels

525 ~~(Enzi and Camuffo, (1995)~~ presented the most complete compilation of pre-instrumental extreme ~~sea level~~water heights  
526 ~~events~~ observed in Venice by reviewing hundreds of historical documents, thus obtaining a sequence of over 100 events  
527 in the 787-1867 period. The long-term evolution has been studied by ~~(Camuffo and Sturaro, (2004)~~ combining  
528 information from documentary sources and instrumental observations. From 1200 to 1740 the flood frequency was  $<0.1$   
529  $\text{yr}^{-1}$ , except for the Spörer period (1500-1540), when it was  $0.63 \text{ yr}^{-1}$ . Subsequently, the frequency increased from  $0.19$   
530  $\text{yr}^{-1}$  in 1830-1930 to  $1.97 \text{ yr}^{-1}$  in 1965-2000. Considering specific thresholds, the number of floods above the 120 cm  
531 threshold has increased from  $1.6 \text{ decade}^{-1}$  (average frequency during the first half of the 20th century) to  $40 \text{ decade}^{-1}$  in  
532 the last decade (2010-2019). Considering a lower (110 cm) threshold the number of events has increased from  $4.2 \text{ decade}^{-1}$   
533 to  $95 \text{ decade}^{-1}$ .

534 Former studies of recent trends (Trigo and Davies, 2002) found that in the second half of the 20<sup>th</sup> century the local ~~mean~~  
535 ~~sea level~~RSL rise compensated for the decreasing frequency of storms, leading to no change in the frequency of floods.  
536 Other studies, found a significant positive trend of moderate ~~surges~~floods in Venice and Trieste during the second half  
537 of the 20th century (1951-1996), that was attributed to increases in the frequency of Sirocco wind conditions over the  
538 central and southern Adriatic (Pirazzoli and Tomasin-Alberto, 2002). A more recent study considered data in the period  
539 1940-2007, reporting a 4% reduction of all- ~~water-height events~~surges, but no significant increase in the frequency or

540 intensity of the most extreme events if the effect of ~~RSLR-RSL rise~~ is subtracted ~~to-from~~ the ~~sea-level~~-data (Lionello *et*  
541 *al.*, 2012b). According to ~~(Ferrarin *et al.*, (2015)~~, the detected increase in amplitude of the tidal waves enhanced the  
542 occurrence of ~~extreme-severe high sea-levels~~water heights in Venice in the period 1940-2014, while changes in storminess  
543 had no significant long-term impact.

544 Observations made in Venice and Chioggia allowed to extend the series of ~~storm-surges~~water-height data back to the  
545 second half of the 18th century (Raicich, 2015). For this longer period, the time series of meteorological surge frequency  
546 ~~did-not~~does not exhibit a significant long-term trend, but strong inter-annual and inter-decadal variability. In summary, the  
547 amount of current evidence shows that while the frequency of floods has clearly progressively increased in time after the  
548 mid-twenty century, there is no clear indication of a sustained trend at multi-decadal time scales in either the frequency  
549 or the severity of extreme ~~meteorological surge events~~surges. The presence of a substantial interannual and interdecadal  
550 variability explains differences among studies, which have considered different periods and different thresholds. -The  
551 long term increase of flood frequency is largely caused by ~~the relative mean sea level~~RSL-rise (connected to both climatic  
552 change and land subsidence; (see Zanchettin *et al* 2020-2021 in this special issue).

553

#### 554 3.2.4.2. Future evolution of extreme ~~sea-levels~~water heights

555 Several past studies considered the future evolution of ~~meteorological storm~~surges and water heights in the Adriatic Sea.  
556 A first analysis was based on a doubled-CO<sub>2</sub> scenario and a single climate simulation (Lionello, Nizzero and Elvini,  
557 2003). Successive studies adopted the SRES scenarios and multiple simulations (Marcos *et al.*, 2011; Lionello, Galati  
558 and Elvini, 2012c; Troccoli *et al.*, 2012; Mel, Sterl and Lionello, 2013). The most recent studies have considered the  
559 whole Mediterranean Sea or large parts of it and an ensemble of simulations for high (RCP8.5) and moderate (RCP4.5)  
560 emission scenarios (Conte and Lionello, 2013; Androulidakis *et al.*, 2015; Vousdoukas *et al.*, 2016; Lionello *et al.*, 2017;  
561 Mentaschi *et al.*, 2017; Vousdoukas *et al.*, 2017; Vousdoukas *et al.*, 2018). These studies are not fully comparable in that  
562 some of them (e.g. Lionello *et al.*, 2017) considered separated contributions from RSL rise and changes of meteorological  
563 surges, whereas others (e.g. Vousdoukas *et al.*, 2017 and 2018) addressed the overall change of sea level extremes.  
564 Further, Vousdoukas *et al.* considered the 100-year return values, while Lionello *et al.* (2017) considered annual maxima  
565 and 5 and 50-year return values. Studies assessing only meteorological surges All studies show a remarkable agreement  
566 on-suggesting non-significant changes or ~~even~~a significant reduction of their intensity ~~of future surges~~, which might  
567 reach about 5% for ~~the RCP8.5 high emissions scenario~~ at the end of the 21st century (with consistent attenuation also of  
568 the wind wave height). This weak climate change signal is consistent with the future prevalent decrease of cyclone  
569 intensity and related wind speeds in the Mediterranean region that is suggested by most studies in spite of model-related  
570 uncertainty and sub-regional differences (see Reale *et al*, 2021 for a recent comprehensive update, and Lionello *et al.*,  
571 2008, Zappa *et al.*, 2013, Nissen *et al.*, 2014, Zappa *et al.* 2015). -However, ~~the~~there is substantial agreement that the  
572 future ~~increase of relative mean sea level has been shown to~~RSL rise will be the dominant factor that will increase  
573 frequency and height of floods (Lionello *et al.*, 2017; Jackson and Jevrejeva, 2016; Jevrejeva *et al.*, 2016; Vousdoukas *et*  
574 *al.*, 2017; Vousdoukas *et al.*, 2018) ~~and it will cause increase of frequency and height of floods~~. Only a very low rate of  
575 future ~~sea-level~~RSL rise, such as that hypothesized in ~~(Troccoli *et al.* (2012)~~, might prevent future increase of floods.  
576 However, such a low future ~~rate of RSL~~ rise is very unlikely (Jordà *et al.*, ~~Gomis and Marcos~~, 2012), because it -It is  
577 lower than the global sea-level rise under the ~~low~~-RCP2.6 scenario in the IPCC SROCC (Oppenheimer *et al.*, 2019) and  
578 it would require ~~relative sea level~~ the RSL rise in Venice during the 21<sup>st</sup> century to be lower than observed during the 20<sup>th</sup>  
579 century (see also Zanchettin *et al.* 2020-2021, in this issue-).

580

581 The future variation of amplitude of tides and surges in response to sea-level rise will depend ~~how the coast is on the~~  
582 ~~adaptation strategy of coastal defences~~ (Bamber and Aspinall, 2013) – protection versus retreat. (Lionello ~~et al., Mufato~~  
583 ~~and Tomasin~~, 2005) showed that a full compensation strategy (protection), preserving the present coastline by dams,  
584 would reduce the amplitude of tides and storm surges, while a no compensation strategy, allowing permanent flooding of  
585 the low coastal areas (retreat), would increase the amplitude of the diurnal components and the amplitude of storm surges  
586 at the North Adriatic coast. ~~These effects are small, but not completely~~ negligible, being about 10% for the diurnal  
587 component in case of 1-m sea-level rise.

588 Projections of extreme sea levels (ESLs) were produced combining dynamic simulations of all relevant components  
589 during the present century, and under RCP4.5 moderate and RCP8.5 high emission scenarios. They include: ~~mean sea-~~  
590 ~~level MSL~~ rise and ~~sea level variations of future anomalies driven by~~ tides, ~~meteorological~~ surges and wind wave set-up  
591 (Vousdoukas *et al.*, 2017; Mentaschi *et al.*, 2017; Vousdoukas *et al.*, 2018), ~~but do not include the effect of local~~  
592 ~~subsidence. MSLs-ESLs~~ were produced through a probabilistic process-based framework (Jackson and Jevrejeva, 2016;  
593 Jevrejeva *et al.*, 2016), incorporating the large uncertainties originating from the Greenland and Antarctic ice sheets under  
594 RCP8.5 high emission scenario (Bamber and Aspinall, 2013). Values for different return periods were estimated using  
595 non-stationary extreme value statistical analysis (Mentaschi *et al.*, 2016) ~~and variations with respect to the 2001-2020~~  
596 ~~baseline~~. Here, the spatially averaged values along the north-west Adriatic coast<sup>5</sup> ~~(i.e. from the Po delta to the Gulf of~~  
597 ~~Trieste) have been extracted from the above datasets, which have pan-European or global coverage are considered.~~

598 The 100-year extreme sea level (100y-ESL) (Figure Fig. 810) ~~at-in~~ the North-West Adriatic Sea<sup>6</sup> by 2050 is very likely  
599 (5-95th percentile) to rise by ~~5-12~~ to ~~23-17~~ cm under the RCP4.5 moderate-emission-mitigation-policy scenario and by  
600 ~~17-26~~ to ~~62-35~~ cm under the RCP8.5 high emissions scenario (Vousdoukas *et al.*, 2018). Similarly, rise to ~~20-38~~~~24-56~~ cm  
601 and ~~48-175~~~~53-171~~ cm, respectively, by the end of the century. ~~By the year 2050, the frequency of present-day 100-year~~  
602 ~~events is projected to increase by 2 or 10 times (i.e. one event per 50 or 10 years) depending on the emissions scenario.~~  
603 ~~By the end of this century, events with the severity of current 1-in-100-year extremes would occur at least every 5 and 1~~  
604 ~~year, under moderate and high emissions, respectively.~~

605 Breaking down the contributing factors to the increase in 100y-ESLs ~~in the North-West Adriatic Sea (Figure Fig. 119),~~  
606 thermal expansion accounts for ~~5845%~~ and ~~3832%~~ (median values) of the projected ~~rise-increase~~ towards the end of the  
607 century, under RCP4.5 moderate and RCP8.5 high emissions, respectively while the Antarctica and Greenland ice sheet  
608 melting contribution vary from ~~145%~~ to ~~203%~~ (median values). However, the combined contributions from ice mass-loss  
609 from glaciers, and ice-sheets in Greenland and Antarctica together, are the dominant factor by 2100, contributing to  
610 ~~5461%~~ and ~~510%~~ (median values) of the 100y-ESL increase under ~~a moderate-emission-mitigation-policy scenario~~  
611 ~~(RCP4.5) and a high emissions scenario (RCP8.5), respectively.~~

612 ~~The increase in 100y ESLs corresponds to more frequent occurrence of present 100y ESL values. By the year 2050, the~~  
613 ~~frequency of present day 100 year events is projected to increase by 2 or 10 times (50 or 10 years) depending on the~~  
614 ~~emissions scenario. By the end of this century, events with the severity of current 1 in 100 year ‘acqua alta’ would occur~~  
615 ~~at least every 5 years under the RCP4.5 and more than once the RCP8.5 scenario, respectively.~~

---

<sup>5</sup> The area in the red box in Figure 1 is from lon 12.1 W to 12.9°W; and from lat 43.8 N and 45.8°N

<sup>6</sup> The area in the box from lon 12.1 W to 12.9°W; and from lat 43.8 N and 45.8°N is considered



616 While the above paragraphs discuss changes due to climatic and meteorological factors, the future dynamics of tides and  
617 surges in response to sea-level rise will also depend on the evolution of the shoreline in the area. As sea levels rise,  
618 societies will have to decide whether to protect the coast and maintain the current shoreline (e.g. with coastal dams), or  
619 allow shoreline retreat. Previous studies (Lionello et al., 2005) have shown that a protection strategy would reduce the  
620 amplitude of tides and storm surges and increase that of Adriatic Sea seiches, while allowing for permanent flooding of  
621 the low coastal areas and retreat, would increase the amplitude of the diurnal tide components and storm surges. These  
622 effects are small, but not negligible, being about 10% for the diurnal component in the case of 1 m RSL rise.

#### 623 4.5. Conclusions and outlook

624 There is a widespread view that ~~extreme sea levels in~~ the floods of the Venice city ~~center~~ are mostly caused by  
625 storm surges and that the actual maximum ~~sea level~~ water height depends substantially on the timing of the storm surge  
626 peak with respect to the phase of the astronomical tide. Consequently, efforts have traditionally focused on the correct  
627 simulation of the intensity, timing and spatial variability of the wind (mainly the Sirocco) for the accurate reproduction  
628 of ~~sea level~~ water height extremes. This review confirms the paramount importance of storm surge, which produced the  
629 highest recorded flood (4 November 1966), but also identifies other phenomena that, though they individually produce  
630 lower ~~sea level~~ water height anomalies than storm surge, can act constructively and yield extreme ~~event~~ water levels. The  
631 event of 12 November 2019 (the second highest ever recorded flood) provides a good example. Therefore, research is  
632 required ~~on~~ PAW surges and meteotsunamis, the other ~~synoptic drivers of contributions to meteorological~~ surges,  
633 including their joint distributions, in order to better understand the likelihood of compound events as that of November  
634 2019. Furthermore, a multivariate statistical model that describes extreme water heights as a function of the various  
635 contributions would provide a more complete characterization of extreme events.

636 ~~Another poorly addressed factor is t~~The ~~actual effect influence~~ of wave-set up ~~and its effect~~ on the ~~sea level~~  
637 ~~anomalies~~ water height inside the Venice lagoon ~~remain uncertain.~~ Some studies have ~~considered~~ computed it during  
638 individual storms affecting Venice (Bertotti and Cavaleri, 1985; Lionello, 1995; De Zolt *et al.*, 2006) and ~~in for~~ 100y-  
639 ESL projections (Vousdoukas *et al.*, 2016; Vousdoukas *et al.*, 2017). ~~These studies show~~ and have shown that the wave  
640 set-up contribution at the Adriatic shoreline can exceed 10 cm, but ~~the its~~ relevance for the flooding of Venice city  
641 ~~center~~ center would require that it initiates sufficiently offshore to affect the sea level at the lagoon inlets. This remains to  
642 be investigated. ~~was never analysed.~~

643 The occurrence of floods, beside from long-term ~~RSLR~~ RSL rise, is modulated by IDAS, sea-level variability at shorter  
644 time scales (from seasonal to decadal). Similarly, also the occurrence of ~~storm~~ meteorological surge ~~events~~ also displays  
645 strong interannual to decadal variability. Evidences linking this variability with astronomical (e.g. the solar cycle) and  
646 climate patterns (e.g. North Hemisphere teleconnections) remain elusive, from both statistical and theoretical approaches.  
647 These issues are important for the development of seasonal predictions of sea-level extremes, understanding of observed  
648 trends and their attribution to long term anthropogenic climate change (and local subsidence). Longer records and better  
649 understanding of the sea-level responses to atmospheric forcing and remote influences would contribute to fill these  
650 knowledge gaps.

651 The synoptic conditions leading to extreme storm surges at Venice are clearly documented, as they are produced by  
652 cyclogenesis occurring in the western Mediterranean Sea. There is consensus on the secondary role that the  
653 meteorological forcing ~~and marine storminess~~ plays in the long-term changes of major floods. This influence Its

654 contribution may decrease further in the future ~~with-because of their~~ projected attenuation ~~of storm surges~~. However, the  
655 confidence on future weakening ~~of storm surges~~ depends on the capability of climate models to correctly reproduce ~~this~~  
656 ~~process~~ the full set of meteorological contributions under climate change. ~~-In addition, including~~ storm surges,  
657 ~~Meteotsunamis and PaW surges do not account for the full atmospheric forcing of extreme sea-level events~~. Literature  
658 on projections of PAW surges and meteotsunamis is presently unavailable and progress on these factors is urgently  
659 required as their changes may ~~have be~~ different signs and magnitude from those of storm surges. Therefore, while  
660 presently available studies agree on the future attenuation of ~~storm-meteorological~~ surges, analyses ~~including~~  
661 ~~all~~ understanding the role of the different meteorological-atmospheric forcings ~~on~~ extreme sea-level events are missing  
662 and deserve investigation.

663 This review confirms the consensus concerning the key control ~~of historic and future RSLR on~~ the frequency and  
664 severity of floods in Venice exerted by historic and future RSL rise. Hence, understanding and predicting the future  
665 evolution of extreme sea-levels water heights in Venice depends critically on the availability of RSL rise ~~R~~ projections  
666 with lower uncertainty than at present. A large fraction of such uncertainty is related to the future emission scenario.  
667 Adopting a moderate-emission-mitigation-policy scenario (RCP2.6), or a high emissions scenario (RCP8.5) would imply  
668 a 30% difference in the projected 100y-ESL at the end of the 21st century. Another major source of uncertainty concerns  
669 the melting of ice-sheets, which accounts for the largest increase of the 100y-ESL at the end of this century, particularly  
670 for a high emission scenario. Further, scenarios for local anthropogenic and long term natural subsidence needs to be  
671 developed, as they can further contribute to the future increase of extreme sea-levels water heights ~~(see~~. Other factors,  
672 such as changes in storminess or the deviation of the Mediterranean mean sea level from that of the Subpolar North  
673 Atlantic (caused by steric effects and redistribution of mass within the Mediterranean Sea) appear to be less important  
674 (see Zanchettin *et al.*, 2020-2021 in this special issue).

675 Reducing uncertainty in the future projections of sea-level-water-height extremes is only one aspect of the research  
676 needed. The other aspect is adaptive planning of coastal defences to consider the large uncertainty ~~on~~ future  
677 evolution, sea-level extremes. A moderate scenario suggests a 10% and 30% increase of 100y-ESL in 2050 and 2100,  
678 respectively. A high emission scenario shows a 25% increase already in 2050, reaching 65% in 2100. These ranges are  
679 further enlarged by the uncertainty in scenario projections (leading to 100y-ESL increase up to 65% and a 160% in 2050  
680 and 2100, respectively), ~~-~~ which should be further expanded to higher values ~~-~~ including high-end ~~RSLR~~ scenarios (see  
681 Zanchettin *et al.*, 2020-2021 in this issue). Further, -the inclusion of uncertainties on future subsidence is required to  
682 assess the likely range of future extreme water heights, which provide the actual information for the hazard to be faced  
683 by coastal defences, the environment of the city and of the lagoon. In other words, the uncertainty range on extreme water  
684 heights is larger than on ESLs and should be detailed at a finer spatial scale. The large range of possible changes,  
685 especially after 2050 is not expected to be reduced substantially in the upcoming years, as it largely relies on human  
686 decisions and pervasive ~~modeling~~ modelling uncertainties, which limits the generation of constrained climate information  
687 and poses major challenges for policy-making decisions on the development of effective adaptation measurements. These  
688 results (see also Lionello *et al.* 2020-2021 in this special issue) stress the need for planning and implementing ~~defence~~  
689 defence strategies of Venice that can be adapted to face the large range of plausible future sea-level extremes.

## 690 Acknowledgements

691 M. Reale has been supported in this work by OGS and Cineca under HPC-TRES award number 2015-07 and by the  
692 project FAIRSEA (Fisheries in the Adriatic Region - a Shared Ecosystem. Approach) funded by the 2014 - 2020 Interreg

693 V-A Italy - Croatia CBC Programme (Standard project ID 10046951).The work of M. Orlic has been supported by  
694 Croatian Science Foundation under the project IP-2018-01-9849 (MAUD). Scientific activity by DZ and GU performed  
695 in the Research Programme Venezia2021, with the contribution of the Provveditorato for the Public Works of Veneto,  
696 Trentino Alto Adige and Friuli Venezia Giulia, provided through the concessionary of State Consorzio Venezia Nuova  
697 and coordinated by CORILA. D. Barriopedro was supported by the Spanish government through the PALEOSTRAT  
698 (CGL2015-69699-R) and JEDiS (RTI2018-096402-BI00) projects.  
699

## 700 **Author contribution**

701 PL coordinated the paper. Specific contributions to the sections are as follows (LA = leading author, CA = contributing  
702 author). Section 1: LA: PL; CA: RJN, DZ. Section 2: LA: MO and FR; CA: PL, GU, CF. Section 3: LA: MR and DB,  
703 CA: FR and PL. Section 4: LA: MV, CA: FR, PL. Section 5: LA: PL, CA: RJN, DZ, DB. Figure 1, [2-3,3,4](#) and [4-5](#) MR,  
704 [Figure 2 PL](#), [Figure 3 GU](#), Figures [5-6,7](#) and [6-8](#) DB; [Figures 7-9](#) and [8-11](#) MV. Table 1:CF; table 2: FR; Appendices:  
705 AI: FR; AII :MR; AIII: DB ; Figure III1 and III2, DB.

706

## 707 **Competing Interest**

708 The authors declare that they have no conflict of interest.

709

## 710 **[5-6](#). Appendix [A1](#): Selected major events**

711 Here we present a short description of extreme sea-level events based on original reports. Each description is based on  
712 the cited sources, which often include synoptic weather maps and diagrams of relevant meteorological parameters (see  
713 table A-1)

### 714 **[A1A.0](#). 15 January 1867**

715 On 15 January 1867, that is just few years before the beginning of regular sea-level records a remarkable storm surge  
716 occurred. Although no tide gauge data are available, contemporary sources reported measurements taken at local  
717 hydrometers.

718 Zantedeschi (1866-67), quoting the local Civil Engineering Office (Ufficio del Genio Civile), reported that the maximum  
719 observed [water](#) height was 1.59 m ‘above the common ordinary high water marked at the royal hydrometer in the Grand  
720 Canal’. The ‘common ordinary high water’ is also known as the ‘comune marino’ (CM), that is the upper edge of the  
721 green belt formed by algae on quays and walls, often indicated by an engraved horizontal mark and/or a ‘C’ (Rusconi,  
722 1983; Camuffo and Sturaro, 2004). According to Dorigo (1961a) the ZMPS is 22.46 cm below the CM of 1825, upon  
723 which the tide gauge zero at S. Stefano was based. Therefore, under the hypothesis that the same CM was adopted at the  
724 royal hydrometer and at S. Stefano, the maximum [RSL-water height](#) should have been approximately 181 cm above  
725 ZMPS.

726 However, later sources gave different [valuesfigures](#). Annali (1941) reported 132 cm above the 1825 CM, therefore the  
727 height would turn out to be 154 cm (153 is reported, maybe due to rounding). Dorigo (1961) also reported 153 cm,  
728 probably quoting Annali (1941).

729 If the 181-cm height was correct, the 1867 height would be the third [highest RL](#)[largest water height](#) ever measured in  
730 Venice, not too far from the 187 cm of 12 November 2019 and the 194 cm reached on 4 November 1966. Note, however,  
731 that in the 1860’s the relative MSL was about 30 cm lower than at present, which makes the 1867 event very remarkable.

732 **A1A.1. 16 April 1936**

733 A cyclone affected the western and central Mediterranean, with a minimum MSLP around 990 hPa in the Gulf of Lions,  
734 causing strong southerly winds blew over the Adriatic. In Venice wind mostly blew from the first quadrant but it veered  
735 to SSW near the surge peak, with gust speed over  $25 \text{ m s}^{-1}$ ; in the meantime the MSLP dropped to 990 hPa.

736 The RSL-water height reached 147 cm; at that time it represented the second highest value ever recorded, the first having  
737 been observed on 15 January 1867 (see Appendix 2 above). The RSL-water-height peak occurred about 2 hr after the  
738 astronomical tide maximum. The meteorological surge contribution was about 914 cm.

739 **A1A.2. 12 November 1951**

740 From 10 to 12 November a deep cyclone formed in the Ligurian Sea where MSLP dropped from 1008 to 984 hPa. On the  
741 Ionian Sea and the Balkans MSLP was higher than 1012 hPa, and the strong MSLP gradient induced strong southerly  
742 winds over the Adriatic Sea, up to over  $20 \text{ m s}^{-1}$  in Venice. As a result, the RSL-water height in Venice increased both  
743 because of the wind-induced surge and the local inverse barometer effect. Luckily, the surge peak occurred at the  
744 astronomical tide minimum. I; if it had occurred at the next high tide, 5 hr later, the observed RSL-water height would  
745 have been about 65 cm higher. The water -heightRSL peak was 151 cm and it exceeded the official danger level of 110  
746 cm for about 9 hr. The meteorological surge peak attained 864 cm.

747 **A1A.3. 4 November 1966**

748 On 3 and 4 November 1966 the MSLP field over the Mediterranean was characterized by a cyclone to the west and an  
749 anticyclone to the east. The cyclone centre deepened and slowly moved from the northwest Mediterranean to northeast  
750 Italy, while the zonal MSLP gradient increased over the Adriatic. As a consequence, strong and persisting southerly wind  
751 affected the Adriatic Sea. In Venice Sirocco speed reached  $20 \text{ m s}^{-1}$  with gusts up to  $28 \text{ m s}^{-1}$ , and the MSLP dropped to  
752 992 hPa.

753 The RSL-water height of 194 cm and the meteorological surge height of 143 cm are the highest values in the whole  
754 instrumental record. The water heightRSL remained over 110 cm for 22 hr. Economic losses for the city of about 400  
755 hundred millions euros have been estimated.

756 Note that two elements limited the water-heightRSL peak, namely the fact that the astronomical tide was negative, though  
757 near zero, at the time of the maximum surge, and that in those days the Moon phase was close to last quarter, making the  
758 astronomical tide amplitude relatively small, around 30 cm. Had the surge peak occurred 5 hr earlier, the water heightRSL  
759 would have attained about 220 cm.

760 **A1A.4. 22 December 1979**

761 This event was connected with a cyclone whose minimum was less than 990 hPa, that moved on 21 and 22 December  
762 from the Algerian coast to the Gulf of Genoa. The combination with higher MSLP over the Balkans enabled southerly  
763 wind blow over the central and southern Adriatic, with gusts up to  $20 \text{ m s}^{-1}$ , while in the northern Adriatic Bora prevailed  
764 with gusts over  $20 \text{ m s}^{-1}$ . The local MSLP was not particularly low (1001 hPa), thus the surge was almost -mainlyentirely  
765 attributed to wind.

766 The meteorological surge peak reached 1068 cm and came 3 hr before the astronomical tide maximum: nevertheless, the  
767 water heightRSL was remarkably high, namely 166 cm which represents the third highest observed value. A water  
768 heightRSL higher than 110 cm lasted for 7 hr.

769 **A1A.5. 1 February 1986**

770 The synoptic situation consisted of cyclone over the western Mediterranean, this time centred in the Gulf of Lions, and  
771 an anticyclone over eastern and northern Europe. A southerly wind flow affected the whole central Mediterranean,  
772 including the Adriatic Sea, but a Bora component was present over the northern Adriatic. Southerly wind was particularly  
773 strong in the southern Adriatic (almost 30 m s<sup>-1</sup> gusts in Bari), while in Venice Bora gusts were faster than 20 m s<sup>-1</sup>.

774 This event is characterised by the fourth highest water heightRSL ever measured in Venice, that is 159 cm. The event  
775 severity was the result of a moderate meteorological surge of 70 cm, that occurred just 1 hr after a 35 cm astronomical  
776 tide maximum and close to the peak of a large seiche. ~~Overall, the surge exceeded 60 cm for 15 hr.~~

777 **A1A.6. 6 November 2000**

778 This event was caused by the combined effect of a large cyclone affecting the whole western Europe and an anticyclone  
779 over eastern Europe. The lowest MSLP was observed in the English Channel with values lower than 970 hPa. The  
780 eastward movement of the cyclone caused the whole Adriatic to experience a remarkable MSLP decrease in the 24 hr  
781 preceding the surge, up to a 27-hPa drop in Venice.

782 As on 1 February 1986, during this event the storm surge and the astronomical tide maximum almost coincided. The  
783 observed water heightRSL attained 144 cm and the surge grew up to ~~89-87~~ cm. The water heightRSL remained above  
784 100 cm for over 7 hr.

785 **A1A.7. 1 December 2008**

786 An intense cyclone, with strong westerly flow affected the western Mediterranean Sea. The day before the surge-flood a  
787 small-scale cyclonic circulation developed over the Gulf of Genoa and moved eastward into the River Po valley. This  
788 caused surface wind over the Tyrrhenian and Adriatic Seas to veer from W to SW, then to S, intensifying in the meantime  
789 and reaching the maximum intensity in the early hours of 1 December. In the afternoon, the cyclonic circulation began  
790 weakening and the intensity of the associated wind in the Adriatic Sea progressively decreased.

791 From the late afternoon of 30 November to the early morning of 1 December, MSLP in Venice dropped by about 13 hPa  
792 in 9 hr, reaching 994 hPa. The wind veered from NNE to SE around 01:30 UTC, with speed between 15 and 20 m s<sup>-1</sup> for  
793 the following 7-8 hr.

794 The water heightRSL attained 156 cm, that is the fifth highest value since 1872. The maximum meteorological surge  
795 height was ~~64-62~~ cm and it occurred less than 1 hr before the astronomical tide maximum.

796 **A1A.8. 29 October 2018**

797 The event was caused by the combined action of a cyclone, centred between the Gulf of Lions and the Gulf of Genoa,  
798 whose minimum MSLP was lower than 985 hPa, and an anticyclone over northeastern and eastern Europe. This  
799 configuration enabled strong Sirocco along the Adriatic, with speed around 15 m s<sup>-1</sup> and gusts up to 25 m s<sup>-1</sup> from the late  
800 morning to the evening in Venice, where MSLP reached a minimum of 996 hPa.

801 The strength and persistence of southerly winds caused the ~~sea level~~meteorological surge to remain particularly high.  
802 The highest water heightRSL was reached at 13:40 UTC with 156 cm (fifth value in the history of the observations in  
803 Venice), a couple of hours later than the astronomical tide maximum, then the water heightRSL decreased to 119 cm at  
804 16:35 UTC at rose again up to 148 cm at 19:25 UTC. The meteorological surge level peaked at ~~92-91~~ cm together with  
805 the maximum water heightRSL and to 117 cm at 19:20 UTC, in coincidence with the astronomical tide minimum. The

806 117 meteorological surge level represents the second highest ever observed and the 119 cm value the highest minimum  
807 water heightRSL. Overall, the water heightRSL was higher than 120 cm for 14 hr, as on 4 November 1966.

### 808 **A1A.9 12, 15 and 17 November 2019**

809 On November 12<sup>th</sup>, 2019, an exceptional flood event took place in Venice, second only to the ~~one that occurred on~~  
810 November 4<sup>th</sup> event, 1966. Moreover, with 15 ~~high tides higher than~~ water heights above 110 cm and 4 ~~events~~-above 140  
811 cm, November 2019 was the worst month for flooding in Venice since the beginning of sea-level records.

812 The extreme high sea level recorded in Venice was due to the combination of the following large-scale and local  
813 dynamics:

- 814 • the in-phase timing between the peak of the atmospheric storm surge and an the lower high-astronomical tide  
815 maximum;
- 816 • the PAW surge produced by a standing low-pressure and wind systems over the Mediterranean Sea ~~that is~~  
817 ~~associated with planetary atmospheric waves trough extending over~~ persisting for the whole month of November  
818 (~~–~~which determined a high monthly mean sea level in the northern Adriatic Sea);
- 819 • the storm surge produced by a deep low-pressure system over the central-southern Tyrrhenian Sea that generated  
820 south-easterly winds along the main axis of the Adriatic Sea, ~~pushing waters to the north~~;
- 821 • the meteotsunamis produced by a fast-moving mesoscale ~~local~~ cyclone travelling in the north-westward direction  
822 ~~over the Adriatic Sea~~ along the Italian coast ~~of the Adriatic Sea, generating a meteotsunami~~;
- 823 • a local set-up produced by very strong south-westerly winds over the Lagoon of Venice, ~~which led to a rise in~~  
824 ~~water levels and damages to the historic city~~.

825 The MSLP minimum of the cyclone on the Tyrrhenian Sea was about 990 hPa. A small deep secondary MSLP minimum  
826 formed in the afternoon, reaching 988 hPa at Venice around 21 UTC. Initially, moderate northeasterly wind was blowing  
827 over the north Adriatic (about 10 m s<sup>-1</sup> at Venice), but between 21 and 22 UTC it veered to S,E then to SW, and sustained  
828 wind reinforced up to 20 m s<sup>-1</sup> at Tessera airport.

829 The highest water heightRSL was reached at 21:50 UTC with 189 cm, that represents the second highest value in the  
830 history of the observations in Venice, and it almost exactly coincided with the astronomical tide peak. The meteorological  
831 surge level peaked at 100 cm, representing the fourth highest value ever observed. The peak water heightRSL was similar  
832 to the 1966 value (namely 194 cm), but, while in 1966 it was mainly the result of a huge meteorological component (143  
833 cm, see A1A.3 above), in 2019 the astronomical tide contribution also played a significant role. Moreover, in 2019 the  
834 relative sea levelRSL was 11 cm higher with respect to 1966.

835 On 15 November another storm surge developed in connection with a large cyclone over west Europe, having a 995 hPa  
836 MSLP minimum over France, and extending into Algeria. Local pressure in Venice reached 1001 hPa and wind blew  
837 from SE at less than 10 m s<sup>-1</sup>. The water heightRSL peaked at 154 cm at 10:40 ~~UTC-UTC, and the surge peak occurred~~  
838 ~~6.5 hours later with 62 cm~~.

### 839 **Appendix B-II: Simulation of the tide- meteorological surge interactions**

840 This short appendix is dedicated to an experiment carried out using the model framework of Cavaleri et al. (2019). Three  
841 different simulations have been performed using only the astronomical tidal forcing (SHYFEM Tide), the meteorological  
842 forcing (SHYFEM Surge) and the full forcing (SHYFEM Total). The difference between the “SHYFEM Total”

843 simulation and the sum of “SHYFEM Surge” and “SHYFEM Tide” represents the effect of the nonlinear interactions  
844 between the astronomical tide and the meteorological surge. Figure B1 shows the results of the simulation and the small  
845 magnitude of the nonlinear effect, which is about only 5% of the total surge in correspondence with the highest peak in  
846 the simulated period.

#### 847 **Appendix C:III Wavelet of the storm surge frequency**

848 In order to integrate the discussion in section 5.3 on the presence of a 11-year periodicity of ~~storm surges~~extreme  
849 detrended water heights, Figures A-1 C1 and A-2 C2 show the amplitude -of the wavelets of the ~~autumn mean~~-time series  
850 of the autumn mean water height Relative Sea Level (RSL) for 1924-2018 and of its daily meteorological surge extremes.  
851 Missing values in the time series before 1928 prevented the computation of the wavelet transform in Fig. C1 for the whole  
852 period 1872-2018 covered with the data. Figure C2 has been limited to the same period for coherence with Fig. C1. In  
853 both graphics, a decadal signal consistent with the 11-year solar cycle is present only for a few decades from the 1970s  
854 to the 1990s and absent before and after this period.

855  
856

#### 857 **References**

858

859 Androulidakis, Y. S., Kombiadou, K. D., Makris, C. V., Baltikas, V. N. and Krestenitis, Y. N.:Storm surges in the  
860 Mediterranean Sea: Variability and trends under future climatic conditions', Dyn. Atmospheres Oceans, 71, pp. 56-82,  
861 2015

862 Bajo, M., Zampato, L., Umgiesser, G., Cucco, A. and Canestrelli, P.: A finite element operational model for storm surge  
863 prediction in Venice. Estuar. Coast. Shelf Sci., 75(1-2), pp.236-249, 2007.

864 Bajo, M., Međugorac, I., Umgiesser, G. and Orlić, M.:Storm surge and seiche modelling in the Adriatic Sea and the  
865 impact of data assimilation', Q. J. R. Meteorol. Soc., 145(722), pp. 2070-2084, 2009

866 Bamber, J. L. and Aspinall, W. P.:An expert judgement assessment of future sea-level rise from the ice sheets', Nat. Clim.  
867 Change, 3(4), pp. 424-427, 2013.

868 Bargagli, A., Carillo, A., Pisacane, G., Ruti, P. M., Struglia, M. V. and Tartaglione, N.:An Integrated Forecast System  
869 over the Mediterranean Basin: Extreme Surge Prediction in the Northern Adriatic Sea', Mon. Weather Rev., 130(5), pp.  
870 1317-1332, 2002

871 Barriopedro, D., García-Herrera, R., Lionello, P. and Pino, C.:A discussion of the links between solar variability and  
872 high-storm-surge events in Venice', J. Geophys. Res. Atmos., 115(13),2010

873 Battistin, D. and Canestrelli, P.:1872-2004 La serie storica delle maree a Venezia, Venice, Italy: Istituzione Centro  
874 Previsioni e Segnalazioni Maree. Available at:  
875 [https://www.comune.venezia.it/sites/default/files/publicCPSM2/pubblicazioni/La\\_serie\\_storica\\_delle\\_maree\\_a\\_Venezi](https://www.comune.venezia.it/sites/default/files/publicCPSM2/pubblicazioni/La_serie_storica_delle_maree_a_Venezi_a_1872-2004_web_ridotto.pdf)  
876 [a\\_1872-2004\\_web\\_ridotto.pdf](https://www.comune.venezia.it/sites/default/files/publicCPSM2/pubblicazioni/La_serie_storica_delle_maree_a_Venezi_a_1872-2004_web_ridotto.pdf), 2006.

877 Bertotti, L., Bidlot, J.-R., Buizza, R., Cavaleri, L. and Janousek, M.:Deterministic and ensemble-based prediction of  
878 Adriatic Sea sirocco storms leading to ‘acqua alta’ in Venice', Q. J. R. Meteorol. Soc., 137(659), pp. 1446-1466, 2011

879 Bertotti, L. and Cavaleri, L.:Coastal set-up and wave breaking', Oceanol. Acta, 8(2), pp. 237-242, 1985

880 Camuffo, D. and Sturaro, G.:Use of proxy-documentary and instrumental data to assess the risk factors leading to sea  
881 flooding in Venice', Glob. Planet. Change, 40(1), pp. 93-103, 2004

- 882 Canestrelli, P., Mandich, M., Pirazzoli, P. A. and Tomasin, A.: Wind, Depressions and Seiche: Tidal Perturbations in  
883 Venice (1951-2000), Venice, Italy: Istituzione Centro Previsioni e Segnalazioni Maree. Available at:  
884 [https://www.comune.venezia.it/sites/default/files/publicCPSM2/pubblicazioni/Venti\\_depressioni\\_e\\_sesse.pdf](https://www.comune.venezia.it/sites/default/files/publicCPSM2/pubblicazioni/Venti_depressioni_e_sesse.pdf), 2001
- 885 Caporin, M. and Fontini, F. : Damages Evaluation, Periodic Floods, and Local Sea Level Rise: The Case of Venice, Italy',  
886 Handbook of Environmental and Sustainable Finance: Elsevier, pp. 93-110, 2016
- 887 Cavaleri, L., Bertotti, L., Buizza, R., Buzzi, A., Masato, V., Umgiesser, G. and Zampieri, M.: Predictability of extreme  
888 meteo-oceanographic events in the Adriatic Sea', Q. J. R. Meteorol. Soc., 136(647), pp. 400-413, 2010
- 889 Cavaleri, L., Bajo, M., Barbariol, F., Bastianini, M., Benetazzo, A., Bertotti, L., Chiggiato, J., Davolio, S., Ferrarin, C.,  
890 Magnusson, L., Papa, A., Pezzutto, P., Pomaro, A. and Umgiesser, G.: The October 29, 2018 storm in Northern Italy - an  
891 exceptional event and its modeling. Prog. Oceanogr. 178, 102178. doi:10.1016/j.pocean.2019.102178., 2019.
- 892 Cavaleri, L., Bajo, M., Barbariol, F., Bastianini, M., Benetazzo, A., Bertotti, L., Chiggiato, J., Ferrarin, C., Trincardi, F.  
893 and Umgiesser, G.: The 2019 Flooding of Venice AND ITS IMPLICATIONS FOR FUTURE PREDICTIONS',  
894 Oceanography, 33(1), pp. 42-49, 2020
- 895 Cerovečki, I., Orlić, M. and Hendershott, M. C. (1997) 'Adriatic seiche decay and energy loss to the Mediterranean', Deep  
896 Sea Research Part I: Oceanographic Research Papers, 44(12), pp. 2007-2029.
- 897 Chiodo, G., Oehrlein, J., Polvani, L. M., Fyfe, J. C. and Smith, A. K.: Insignificant influence of the 11-year solar cycle  
898 on the North Atlantic Oscillation', Nat. Geosci., 12(2), pp. 94-99, 2019.
- 899 Clette, F., Svalgaard, L., Vaquero, J. M., and Cliver, E. W.: Revisiting the sunspot number. Space Sci. Rev., 186(1), 35-  
900 103, 2014.
- 901 Codiga, D. L.: Unified tidal analysis and prediction using the UTide Matlab functions. Graduate School of Oceanography,  
902 University of Rhode Island Narragansett, RI., 2011
- 903 Conte, D. and Lionello, P.: Characteristics of large positive and negative surges in the Mediterranean Sea and their  
904 attenuation in future climate scenarios', Glob. Planet. Change, 111, pp. 159-173, 2013.
- 905 De Zolt, S., Lionello, P., Nuhu, A. and Tomasin, A.: The disastrous storm of 4 November 1966 on Italy', Nat. Hazards  
906 Earth Syst. Sci. , 6(5), pp. 861-879, 2006.
- 907 Dorigo, L.: Le osservazioni mareografiche in Laguna di Venezia, Venice, Italy: Istituto Veneto di Scienze, Lettere e Arti,  
908 2061a.
- 909 Dorigo, L.: Maree eccezionali registrate a Venezia Punta della Salute. Periodo 1867-1960: Istituto Veneto di Scienze,  
910 Lettere e Arti, 2061b
- 911 Enzi, S. and Camuffo, D.: Documentary sources of the sea surges in Venice from ad 787 to 1867', Natural Hazards, 12(3),  
912 pp. 225-287, 1995.
- 913 Fagherazzi, S., Fossier, G., D'Alpaos, L. and D'Odorico, P.: Climatic oscillations influence the flooding of Venice',  
914 Geophysical Research Letters, 32(19), 2005.
- 915 Ferrarin, C., Maicu, F. and Umgiesser, G.: The effect of lagoons on Adriatic Sea tidal dynamics', Ocean Modelling, 119,  
916 pp. 57-71, 2017.



- 917 Ferrarin, C., Tomasin, A., Bajo, M., Petrizzo, A. and Umgiesser, G.: 'Tidal changes in a heavily modified coastal wetland',  
918 Cont. Shelf Res., 101, pp. 22-33, 2015.
- 919 Ferrarin, C., Bajo, M., Benetazzo, A., Cavalari, L., Chiggiato, J., Davison, S., Davolio, S., Lionello, P., Orlić, M.,  
920 Umgiesser, G. (2020b). "Local and large-scale controls of the exceptional Venice floods of November 2019", submitted  
921 to Progress in Oceanography.
- 922 Ferrarin, C., Bajo, M., Benetazzo, A., Cavaleri, L., Chiggiato, J., Davison, S., Davolio, S., Lionello, P., Orlić, M.,  
923 Umgiesser, G.: Local and large-scale controls of the exceptional Venice floods of November 2019, Progress in  
924 Oceanography, submitted, 2021.
- 925 Flaounas E., Fanni Dora Kelemen, Heini Wernli, Miguel Angel Gaertner, Marco Reale, Emilia Sanchez-Gomez, Piero  
926 Lionello, Sandro Calmanti, Zorica Podrascanin, Samuel Somot, Naveed Akhtar, Raquel Romera, Dario Conte:  
927 Assessment of an ensemble of ocean-atmosphere coupled and uncoupled regional climate models to reproduce the  
928 climatology of Mediterranean cyclones. Clim. Dyn.51:3, pages 1023-1040, 2018.
- 929 Franco, P., jeftić, L., Malanotte Rizzoli, P., Orlić, M. and Purga, N.: Descriptive Model of the Northern Adriatic',  
930 Oceanol. Acta, 5(3), pp. 11, 1982.
- 931 Garrido-Perez, J. M., Ordóñez, C., Barriopedro, D., García-Herrera, R. and Paredes, D.: Impact of weather regimes on  
932 wind power variability in western Europe', Applied Energy, 264, pp. 114731. Gregory, J. M., Griffies, S. M., Hughes, C.  
933 W., Lowe, J. A., Church, J. A., Fukimori, I., Gomez, N., Kopp, R.E., Landerer, F., Le Cozannet, G., Ponte, R.M.,  
934 Stammer, D., Tamisiea, M.E. and van de Wal, R. S. (2019). Concepts and terminology for sea level: Mean, variability  
935 and change, both local and global. Surv. Geophys., 40(6), 1251-1289, 2020.
- 936 Hendershott, M. C. and Speranza, A.: 'Co-oscillating tides in long, narrow bays; the Taylor problem revisited', Deep-Sea  
937 Res. Oceanogr. Abstr. [, 18(10), pp. 959-980, 1971.
- 938 Hersbach, H., Bell, B., Berrisford, P., Hirahara, S., Horányi, A., Muñoz-Sabater, J., Nicolas, J., Peubey, C., Radu, R. and  
939 Schepers, D.: 'The ERA5 global reanalysis', Q. J. R. Meteorol. Soc., 146(730), pp. 1999-2049, 2020.
- 940 Horsburgh, K. J. and Wilson, C.: Tide-surge interaction and its role in the distribution of surge residuals in the North Sea.  
941 J. Geophys. Res. Oceans., 112(C8), 2007.
- 942 ISPRA, C. a. and CNR-ISMAR: Un mese di alte maree eccezionali. Dinamica e anomalia dell'evento del 12 novembre  
943 2019. Available at: [www.comune.venezia.it/content/le-acque-alte-eccezionali](http://www.comune.venezia.it/content/le-acque-alte-eccezionali) (Accessed: 30 September 2019), 2020.
- 944 Jackson, L. P. and Jevrejeva, S.: A probabilistic approach to 21st century regional sea-level projections using RCP and  
945 High-end scenarios', Glob. Planet. Change, 146, pp. 179-189, 2016.
- 946 Janeković, I. and Kuzmić, M.: 'Numerical simulation of the Adriatic Sea principal tidal constituents', Ann. Geophys.,  
947 23(10), pp. 3207-3218, 2005.
- 948 Jansa, A., Alpert, P., Buzzi, A. and Arbogast, P.: MEDEX, cyclones that produce high impact weather in the  
949 Mediterranean', Available at <http://medex.aemet.uib.es>, 2001.
- 950 Jevrejeva, S., Jackson, L. P., Riva, R. E. M., Grinsted, A. and Moore, J. C.: Coastal sea level rise with warming above 2  
951 °C', Proc. Natl. Acad. Sci., 113(47), pp. 13342-13347, 2016.
- 952 Jordà, G., Gomis, D. and Marcos, M.: Comment on "Storm surge frequency reduction in Venice under climate change"  
953 by Troccoli et al', Clim. Change, 113(3-4), pp. 1081-1087, 2012.
- 954 Karabeg, M. and Orlić, M.: The influence of air pressure on sea level in the North Adriatic—a frequency-domain  
955 approach', Acta Adriat., 23(1/2), pp. 21-27, 1982.

- 956 Lionello, P.: Oceanographic prediction for the Venetian Littoral', *NUOVO CIMENTO DELLA SOCIETA ITALIANA*  
957 *DI FISICA C-GEOPHYSICS AND SPACE PHYSICS*, 18(3), pp. 245-268, 1995.
- 958 Lionello, P., Dalan, F. and Elvini, E.: Cyclones in the Mediterranean region: the present and the doubled CO2 climate  
959 scenarios', *Clim. Res.*, 22(2), pp. 147-159, 2002.
- 960 Lionello, P., Nizzero, A. and Elvini, E.: A procedure for estimating wind waves and storm-surge climate scenarios in a  
961 regional basin: The Adriatic Sea case', *Clim. Res.*, 23(3), pp. 217-231, 2003.
- 962 Lionello, P.: Extreme storm surges in the gulf of venice: Present and future climate', *Flooding and Environmental*  
963 *Challenges for Venice and its Lagoon: State of Knowledge.*, pp. 59-69, 2005
- 964 Lionello, P., Mufato, R. and Tomasin, A.: Sensitivity of free and forced oscillations of the Adriatic Sea to sea level rise',  
965 *Clim. Res.*, 29(1), pp. 23-39, 2005.
- 966 Lionello, P., Sanna, A., Elvini, E., and Mufato, R.: A data assimilation procedure for operational prediction of storm surge  
967 in the northern Adriatic Sea. *Cont. Shelf Res.*, 26(4), 539-553, 2006.
- 968 Lionello, P., Bhend, J., Buzzi, A., Della-Marta, P. M., Krichak, S. O., Jansa, A., Maheras, P., Sanna, A., Trigo, I. F. and  
969 Trigo, R.: Cyclones in the Mediterranean region: climatology and effects on the environment', *Developments in earth*  
970 *and environmental sciences: Elsevier*, pp. 325-372, 2006a.
- 971 Lionello, P., Bhend, J., Buzzi, A., Della-Marta, P. M., Krichak, S. O., Jansà, A., Maheras, P., Sanna, A., Trigo, I. F. and  
972 Trigo, R.: Chapter 6 Cyclones in the Mediterranean region: Climatology and effects on the environment. *Developments*  
973 *in Earth and Environmental Sciences*, 2006b.
- 974 Lionello, P., Boldrin, U., and Giorgi, F.: Future changes in cyclone climatology over Europe as inferred from a regional  
975 climate simulation. *Clim. Dyn.*, 30(6), 657-671, 2008.
- 976 Lionello, P., Abrantes, F., Congedi, L., Dulac, F., Gacic, M., Gomis, D., Goodess, C., Hoff, H., Kutiel, H., Luterbacher,  
977 J., Planton, S., Reale, M., Schröder, K., Vittoria Struglia, M., Toreti, A., Tsimplis, M., Ulbrich, U. and Xoplaki, E.:  
978 'Introduction: Mediterranean climate-background information', *The Climate of the Mediterranean Region*, pp. xxxv-xc,  
979 2012a
- 980 Lionello, P., Cavaleri, L., Nissen, K. M., Pino, C., Raicich, F. and Ulbrich, U.: Severe marine storms in the Northern  
981 Adriatic: Characteristics and trends', *Phys. Chem. Earth*, 40-41, pp. 93-105, 2012b.
- 982 Lionello, P., Galati, M. B. and Elvini, E.: Extreme storm surge and wind wave climate scenario simulations at the Venetian  
983 littoral', *Phys. Chem. Earth*, 40-41, pp. 86-92, 2012c.
- 984 Lionello, P., Conte, D., Marzo, L. and Scarascia, L.: 'The contrasting effect of increasing mean sea level and decreasing  
985 storminess on the maximum water level during storms along the coast of the Mediterranean Sea in the mid 21st century',  
986 *Glob. Planet. Change*, 151, pp. 80-91, 2017.
- 987 Lionello, P., Trigo, I. F., Gil, V., Liberato, M. L. R., Nissen, K. M., Pinto, J. G., Raible, C. C., Reale, M., Tanzarella, A.,  
988 Trigo, R. M., Ulbrich, S. and Ulbrich, U.: Objective climatology of cyclones in the Mediterranean region: A consensus  
989 view among methods with different system identification and tracking criteria', *Tellus, Series A: Dynamic Meteorology*  
990 *and Oceanography*, 68(1), 2016.
- 991 Lionello, P., Conte, D. and Reale, M.: The effect of cyclones crossing the Mediterranean region on sea level anomalies  
992 on the Mediterranean Sea coast', *Nat. Hazards Earth Syst. Sci.*, 19(7), pp. 1541-1564, 2019.

- 993 Lionello, P., Nicholls, J.R., Umgiesser, G., Zanchettin, D.: Venice flooding and sea level: past evolution, present issues  
994 and future projections' *Nat. Hazards Earth Syst. Sci.* (submitted), 2021
- 995 Livio, D.: *Le alte maree eccezionali a Venezia*, Venice, Italy: Ufficio Idrografico del Magistrato alle Acque (156), 1968.
- 996 Lovato, T., Androsov, A., Romanenkov, D., & Rubino, A.: The tidal and wind induced hydrodynamics of the composite  
997 system Adriatic Sea/Lagoon of Venice. *Cont. Shelf Res.*, 30(6), 692-706, 2010.
- 998 Malačić, V., Viezzoli, D. and Cushman-Roisin, B.: Tidal dynamics in the northern Adriatic Sea', *J. Geophys. Res.*  
999 *Oceans.*, 105(C11), pp. 26265-26280, 2000.
- 1000 Manca, B., Masetti, F. and Zennaro, P. *Analisi spettrale delle seste dell'Adriatico.*, *Boll. di Geofis. Teor. ed Appl.*, 16,  
1001 pp. 10, 1974.
- 1002 Marcos, M., Jordà, G., Gomis, D. and Pérez, B.: Changes in storm surges in southern Europe from a regional model under  
1003 climate change scenarios', *Glob. Planet. Change*, 77(3), pp. 116-128, 2011.
- 1004 Markowsky, P., Richardson, Y.: *Mesoscale Meteorology in Midlatitudes*, Wiley-Blackwell, Chichester, 407 pp., 2010
- 1005 Martínez-Asensio, A., Marcos, M., Tsimplis, M. N., Gomis, D., Josey, S. and Jordà, G.: Impact of the atmospheric climate  
1006 modes on Mediterranean sea level variability', *Glob. Planet. Change*, 118, pp. 1-15, 2014.
- 1007 Martínez-Asensio, A., Tsimplis, M. N. and Calafat, F. M.: Decadal variability of European sea level extremes in relation  
1008 to the solar activity', *Geophys. Res. Lett.*, 43(22), pp. 11,744-11,750, 2016.
- 1009 Mel, R., Carniello, L. and D'Alpaos, L.: Dataset of wind setup in a regulated Venice lagoon', *Data in brief*, 26, pp. 104386,  
1010 2019.
- 1011 Mel, R., Sterl, A. and Lionello, P.: High resolution climate projection of storm surge at the Venetian coast', *Nat. Hazards*  
1012 *Earth Syst. Sci.*, 13(4), pp. 1135-1142, 2013.
- 1013 Mel, R. and Lionello, P.: Storm surge ensemble prediction for the city of Venice. *WeatherForecast.*, 29(4), 1044-1057,  
1014 2014.
- 1015 Mentaschi, L., Vousdoukas, M., Voukouvalas, E., Sartini, L., Feyen, L., Besio, G. and Alfieri, L.: The transformed-  
1016 stationary approach: a generic and simplified methodology for non-stationary extreme value analysis', *Hydrol. Earth Syst.*  
1017 *Sci.*, 20(9), pp. 3527-3547, 2016.
- 1018 Mentaschi, L., Vousdoukas, M. I., Voukouvalas, E., Dosio, A. and Feyen, L.: Global changes of extreme coastal wave  
1019 energy fluxes triggered by intensified teleconnection patterns', *Geophys. Res. Lett.*, 44(5), pp. 2416-2426, 2017.
- 1020 Međugorac, I., Pasarić, M. and Orlić, M. Two recent storm-surge episodes in the Adriatic', *Int. J. Saf. Secur. Eng.*, 6, pp.  
1021 8, 2016.
- 1022 Međugorac, I., Orlić, M., Janeković, I., Pasarić, Z. and Pasarić, M.: Adriatic storm surges and related cross-basin sea-  
1023 level slope', *J. Mar. Syst.* *J Mar Syst*, 181, pp. 79-90, 2018.
- 1024 Neu, U., Akperov, M. G., Bellenbaum, N., Benestad, R., Blender, R., Caballero, R., Coccozza, A., Dacre, H. F., Feng, Y.,  
1025 Fraedrich, K., Grieger, J., Gulev, S., Hanley, J., Hewson, T., Inatsu, M., Keay, K., Kew, S. F., Kindem, I., Leckebusch,  
1026 G. C., Liberato, M. L. R., Lionello, P., Mokhov, I. I., Pinto, J. G., Raible, C. C., Reale, M., Rudeva, I., Schuster, M.,  
1027 Simmonds, I., Sinclair, M., Sprenger, M., Tilinina, N. D., Trigo, I. F., Ulbrich, S., Ulbrich, U., Wang, X. L. and Wernli,  
1028 H. : Imilast: A community effort to intercompare extratropical cyclone detection and tracking algorithms', *Bull. Am.*  
1029 *Meteorol. Soc.*, 94(4), pp. 529-547, 2013.

- 1030 Nissen, K. M., Leckebusch, G. C., Pinto, J. G., and Ulbrich, U. (2014). Mediterranean cyclones and windstorms in a  
1031 changing climate. *Regional Environmental Change*, 14(5), 1873-1890.
- 1032 Oppenheimer, M., Glavovic, B., Hinkel, J., Van de Wal, R., Magnan, A. K., Abd-Elgawad, A., Cai, R., Cifuentes-Jara,  
1033 M., Deconto, R. M. and Ghosh, T.: Sea level rise and implications for low-lying islands, coasts and communities IPCC  
1034 Special Report on the Ocean and Cryosphere in a Changing Climate ed HO Pörtner et al., 2019.
- 1035 Orlić, M.: On the frictionless influence of planetary atmospheric waves on the Adriatic sea level, *J. Phys. Oceanogr.*, 13,  
1036 1301-1306, 1983.
- 1037 Orlić, M.: Anatomy of sea level variability-an example from the Adriatic', *The Ocean Engineering Handbook: CRC*  
1038 *Press*, 2001.
- 1039 Pasarić, M. and Orlić, M.: Long-term meteorological preconditioning of the North Adriatic coastal floods', *Cont. Shelf*  
1040 *Res.*, 21(3), pp. 263-27, 2001.
- 1041 Pirazzoli, P. A. and Tomasin, A.: Recent Evolution of Surge-Related Events in the Northern Adriatic Area', *J. Coast.*  
1042 *Res.*, 18(3), pp. 537-554, 2001.
- 1043 Raichich, F. : Long-term variability of storm surge frequency in the Venice Lagoon: an update thanks to 18th century sea  
1044 level observations', *Nat. Hazards Earth Syst. Sci.*, 15(3), pp. 527-535, 2015.
- 1045 Reale, M., Liberato, M. L. R., Lionello, P., Pinto, J. G., Salon, S. and Ulbrich, S.: A global climatology of explosive  
1046 cyclones using a multi-tracking approach', *Tellus A: Dynamic Meteorology and Oceanography*, 71(1), pp. 1611340, 2019.
- 1047 Reale, M. and Lionello, P.: Synoptic climatology of winter intense precipitation events along the Mediterranean coasts',  
1048 *Nat. Hazards Earth Syst. Sci.*, 13(7), pp. 1707-1722, 2013.
- 1049 Reale, M., Cabos, W., Cavicchia, L., Conte, D. Coppola, E., Flaounas, E., Giorgi, F., Hochman, A., Li, L., Lionello, P.,  
1050 Podrascanin, Z., Sanchez Gomez, E., Scoccimarro, E., Sein, D. Somot, S.: Future projections of Mediterranean cyclone  
1051 characteristics using the Med-CORDEX ensemble of coupled regional climate system models', *Clim. Dyn.*, submitted,  
1052 2021
- 1053 Robinson, A. R., Tomasin, A. and Artegiani, A.: Flooding Venice phenomenology and prediction of the Adriatic Storm  
1054 surge', *Q. J. R. Meteorol. Soc.*, 99(422 (OCTOBER, 1973)), pp. 688-692, 1973.
- 1055 Roland, A., Cucco, A., Ferrarin, C., Hsu, T.-W., Liau, J.-M., Ou, S.-H., Umgiesser, G. and Zanke, U.: On the development  
1056 and verification of a 2-D coupled wave-current model on unstructured meshes', *J. Mar. Syst.*, 78, pp. S244-S254, 2009.
- 1057 Sarretta, A., Pillon, S., Molinaroli, E., Guerzoni, S., Fontolan, G.: Sediment budget in the Lagoon of Venice, Italy', *Cont.*  
1058 *Shelf Res.* 30:934–949. DOI: 10.1016/j.csr.2009.07.002, 2010.
- 1059 Šepić, J., Vilibić, I. and Belušić, D.: 2009 Source of the 2007 Ist meteotsunami (Adriatic Sea)', *J. Geophys. Res. Oceans.*,  
1060 114(C3), 2009.
- 1061 Thiéblemont, R., Matthes, K., Omrani, N.-E., Kodera, K. and Hansen, F. : Solar forcing synchronizes decadal North  
1062 Atlantic climate variability', *Nature Communications*, 6(1), pp. 8268, 2015.
- 1063 Tomasin, A.: The frequency of Adriatic surges and solar activity.: Istituto Studio Dinamica Grandi Masse (ISDGM-  
1064 CNR), 2002.
- 1065 Tomasin, A., and Frassetto, R.: Cyclogenesis and forecast of dramatic water elevations in Venice. In Elsevier  
1066 *Oceanography Series*, 25, pp. 427-438) Elsevier, 1979.

- 1067 Toreti, A., Xoplaki, E., Maraun, D., Kuglitsch, F.-G., Wanner, H. and Luterbacher, J.: Characterisation of extreme winter  
1068 precipitation in Mediterranean coastal sites and associated anomalous atmospheric circulation patterns', *Nat. Hazards*  
1069 *Earth Syst. Sci.*, 10(5), pp. 1037-1050, 2010.
- 1070 Trigo, I. F., Bigg, G. R. and Davies, T. D.: 2002 Climatology of Cyclogenesis Mechanisms in the Mediterranean', *Mon.*  
1071 *Weather Rev.*, 130(3), pp. 549-569, 2002.
- 1072 Trigo, I. F. and Davies, T. D.: Meteorological conditions associated with sea surges in Venice: a 40 year climatology',  
1073 *International Journal of Climatology*, 22(7), pp. 787-803, 2002.
- 1074 Trigo, I. F., Davies, T. D. and Bigg, G. R.: Objective climatology of cyclones in the Mediterranean region', *J. Clim.*,  
1075 12(6), pp. 1685-1696, 1999.
- 1076 Troccoli, A., Zambon, F., Hodges, K. I. and Marani, M.: Storm surge frequency reduction in Venice under climate  
1077 change', *Clim. Change*, 113(3-4), pp. 1065-1079, 2012.
- 1078 Ulbrich, U., Leckebusch, G. C., Grieger, J., Schuster, M., Akperov, M., Bardin, M. Y., Feng, Y., Gulev, S., Inatsu, M.,  
1079 Keay, K., Kew, S. F., Liberato, M. L. R., Lionello, P., Mokhov, I. I., Neu, U., Pinto, J. G., Raible, C. C., Reale, M.,  
1080 Rudeva, I., Simmonds, I., Tilinina, N. D., Trigo, I. F., Ulbrich, S., Wang, X. L. and Wernli, H.: Are Greenhouse Gas  
1081 Signals of Northern Hemisphere winter extra-tropical cyclone activity dependent on the identification and tracking  
1082 algorithm?', *Meteorologische Zeitschrift*, 22(1), pp. 61-68, 2013.
- 1083 Ulbrich, U., Leckebusch, G. C. and Pinto, J. G.: Extra-tropical cyclones in the present and future climate: a review',  
1084 *Theoretical and Applied Climatology*, 96(1-2), pp. 117-131, 2009.
- 1085 Ulbrich, U., Lionello, P., Belušić, D., Jacobeit, J., Knippertz, P., Kuglitsch, F. G., Leckebusch, G. C., Luterbacher, J.,  
1086 Maugeri, M., Maheras, P., Nissen, K. M., Pavan, V., Pinto, J. G., Saaroni, H., Seubert, S., Toreti, A., Xoplaki, E. and Ziv,  
1087 B.: Climate of the mediterranean: Synoptic patterns, temperature, precipitation, winds, and their extremes', *The Climate*  
1088 *of the Mediterranean Region*, pp. 301-346, 2012.
- 1089 Umgiesser, G., Canu, D. M., Cucco, A. and Solidoro, C.: A finite element model for the Venice Lagoon. Development,  
1090 set up, calibration and validation', *J. Mar. Syst.*, 51(1-4), pp. 123-145, 2004.
- 1091 Umgiesser, G. et al.: The prediction of floods in Venice: methods, models and uncertainty", *Nat. Hazards Earth Syst. Sci.*  
1092 (submitted), 2021
- 1093 Vilibić, I. and Šepić, J.: Destructive meteotsunamis along the eastern Adriatic coast: Overview', *Phys. Chem. Earth, Parts*  
1094 *A/B/C*, 34(17), pp. 904-917, 2009.
- 1095 Vousdoukas, M. I., Mentaschi, L., Voukouvalas, E., Verlaan, M. and Feyen, L.: Extreme sea levels on the rise along  
1096 Europe's coasts', *Earth's Future*, 5(3), pp. 304-323, 2017.
- 1097 Vousdoukas, M. I., Mentaschi, L., Voukouvalas, E., Verlaan, M., Jevrejeva, S., Jackson, L. P. and Feyen, L.: 'Global  
1098 probabilistic projections of extreme sea levels show intensification of coastal flood hazard', *Nature Communications*,  
1099 9(1), pp. 2360, 2018.
- 1100 Vousdoukas, M. I., Voukouvalas, E., Annunziato, A., Giardino, A. and Feyen, L.: Projections of extreme storm surge  
1101 levels along Europe', *Clim. Dyn.*, 47(9), pp. 3171-3190, 2016.
- 1102 Zanchettin, D., Rubino, A., Traverso, P. and Tomasino, M.: Teleconnections force interannual-to-decadal tidal variability  
1103 in the Lagoon of Venice (northern Adriatic)', *J. Geophys. Res. Atmos.*, 114(7), 2009.
- 1104 Zanchettin, D. et al.: Sea-level rise in Venice: historic and future trends, *Nat. Hazards Earth Syst. Sci.* (submitted), 2021.

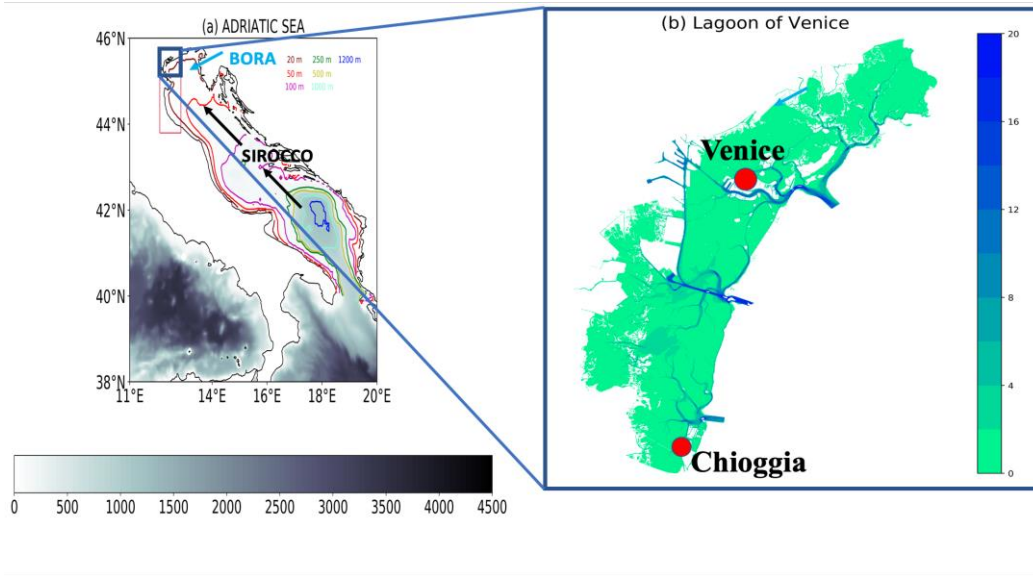
1105 Zappa, G., Shaffrey, L. C., Hodges, K. I., Sansom, P. G., and Stephenson, D. B.: A multimodel assessment of future  
1106 projections of North Atlantic and European extratropical cyclones in the CMIP5 climate models. *J. Clim.*, 26(16), 5846-  
1107 5862, 2013.

1108 Zappa, G., Hawcroft, M. K., Shaffrey, L., Black, E., and Brayshaw, D. J.: Extratropical cyclones and the projected decline  
1109 of winter Mediterranean precipitation in the CMIP5 models. *Clim. Dyn.*, 45(7), 1727-1738, 2015.

1110

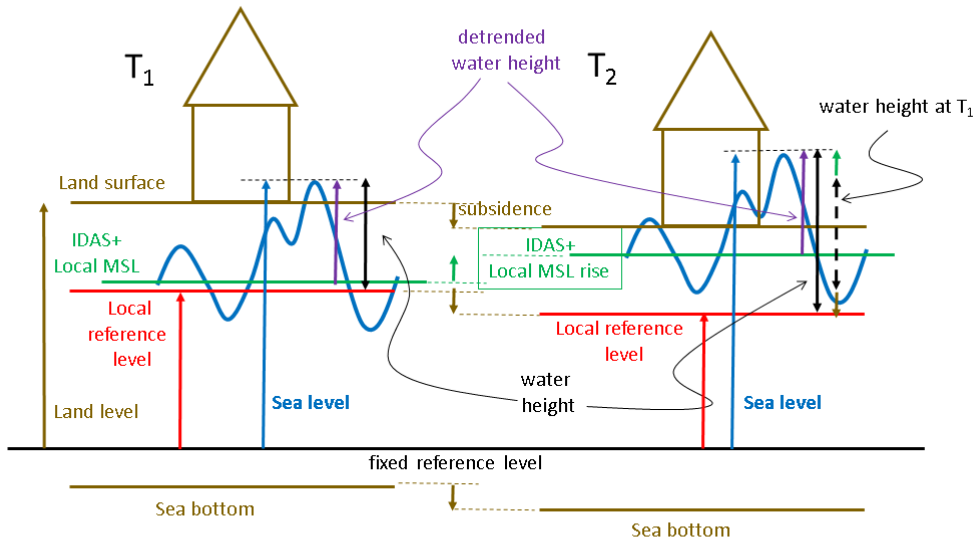
1111  
|

1112



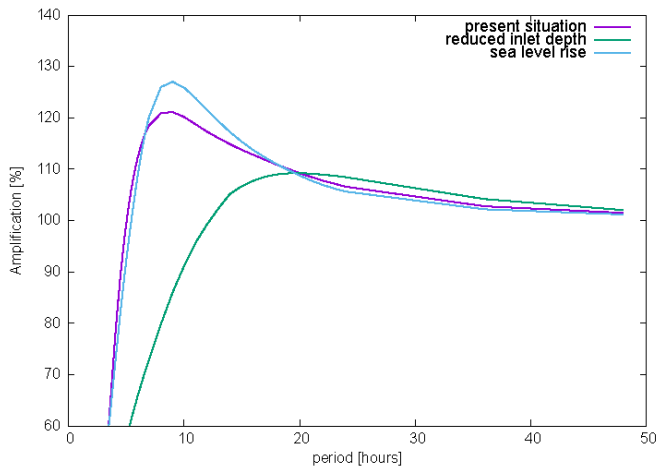
1113

1114 **Figure 1: left panel: bathymetry of the Adriatic Sea with the position of Venice and arrows denoting the directions of the two**  
 1115 **main wind regimes affecting the North Adriatic. The red box (whose northern part includes the whole lagoon) denotes the area**  
 1116 **represented by the data in Figs.8 and 9. Right panel: morphology of the lagoon of Venice with the three inlets connecting it to**  
 1117 **the Adriatic Sea, and the position of the city and of Chioggia (the bathymetric data are for year 2002 and are based on original**  
 1118 **data provided by Magistrato alla Acque di Venezia and elaborated by Sarretta et al. (2010).**



1119

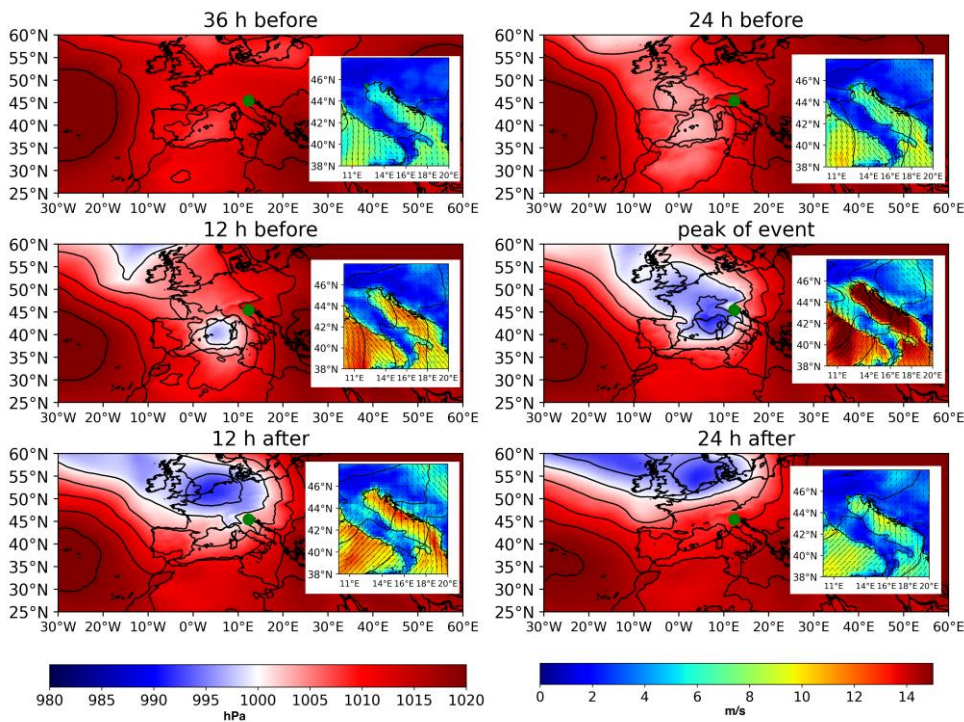
1120 **Figure 2 schematic showing changes of water height for a hypothetical identical event occurring at time  $T_1$  (mid of 20<sup>th</sup> century)**  
 1121 **and  $T_2$  (first decades of the 21<sup>st</sup> century). Local subsidence has shifted to a lower level the land surface, the reference level and**  
 1122 **the sea bottom. RSL rise and IDAS have shifted to an upper level the sea surface. The water height of the same event**  
 1123 **hypothetically measured at  $T_1$  and  $T_2$  differ by the IDAS and RSL rise contribution. The latter is split in local subsidence and**  
 1124 **mean sea level rise. The detrended water height is the addition of the meteorological surge (Storm surge, PAW surge,**  
 1125 **meteotsunamis), astronomical tide and seiches.**



1126

1127  
1128  
1129  
1130

**Figure 3 Amplification (percentage, y-axis, values higher/lower than 100 correspond to amplification/attenuation) of sea level oscillations in the Venice city centre with respect to their amplitude at the lagoon inlets as a function of their period (hours, x-axis). The curves show the present situation (violet), a hypothetical reduction to 6 meters of the depth of the three inlets of the lagoon (green), a RSL rise of 1 meter without any change in the morphology of the lagoon.**

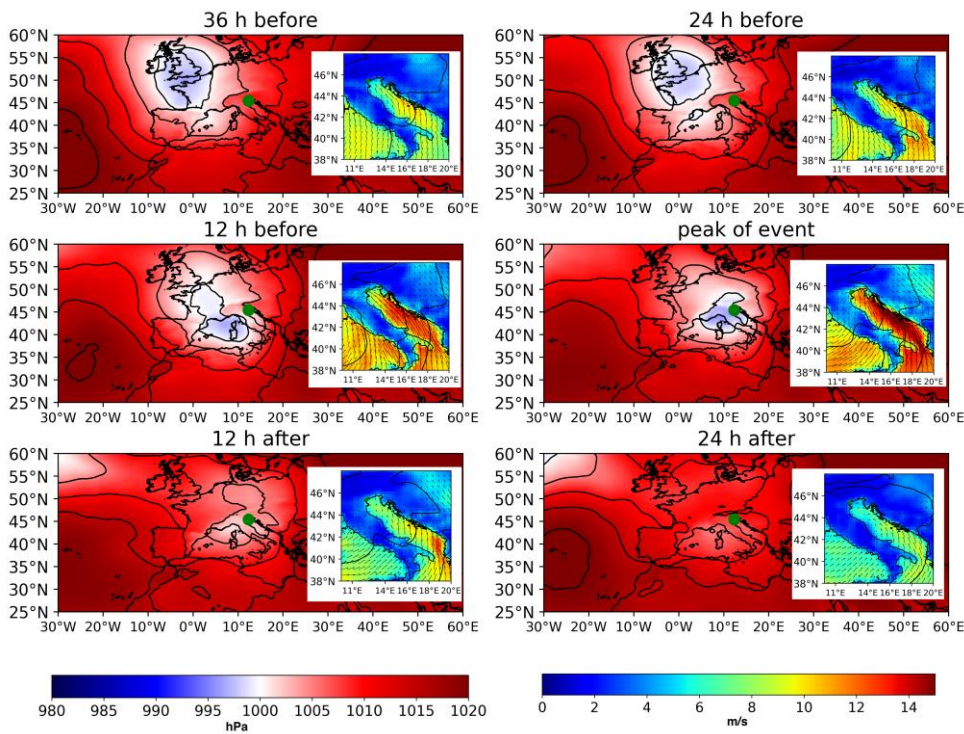


1131

1132  
1133  
1134  
1135

**Figure 2-4 large panels show -the cComposite of MSLP fields based on ERA5 (in hPa, left color bar) datasets associated with storm surges higher than 50 cm in Venice (see table 1). Small panels show the corresponding wind fields over the Adriatic Sea (m/s, right color bar). The time lags chosen for the composites is 36, 24, 12 hours before and 12, 24 hours after the peak of the event. The gGreen dot shows the location of the city of Venice**

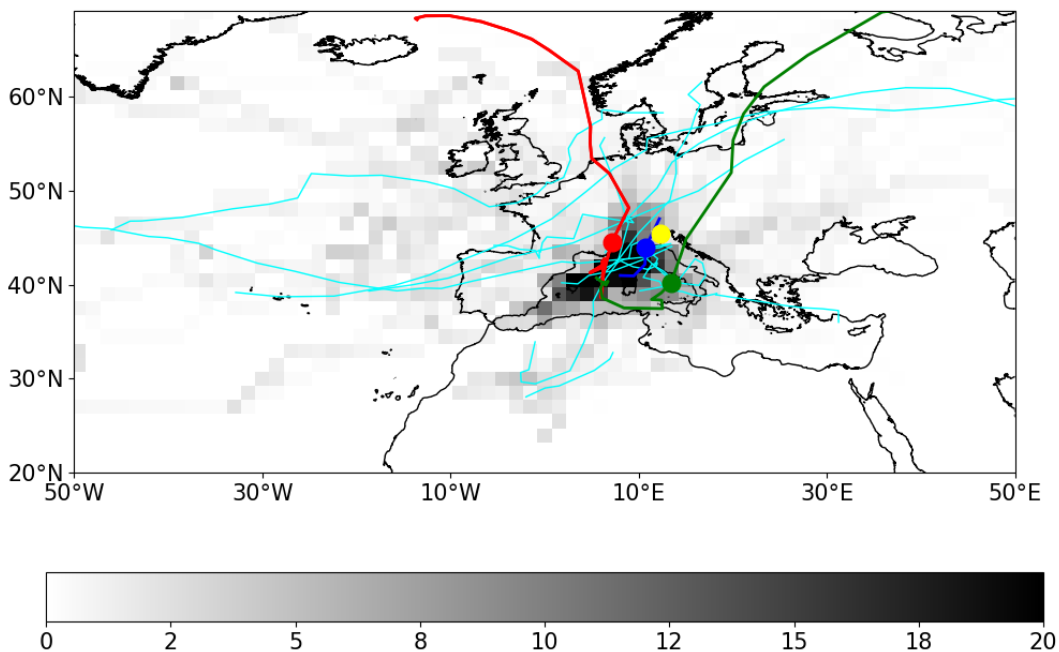




1136

1137

Figure 5-3- Same as figure 2, except it is based on the events in table 1 with storm surge height lower than 50cm



1138

1139

1140

1141

1142

1143

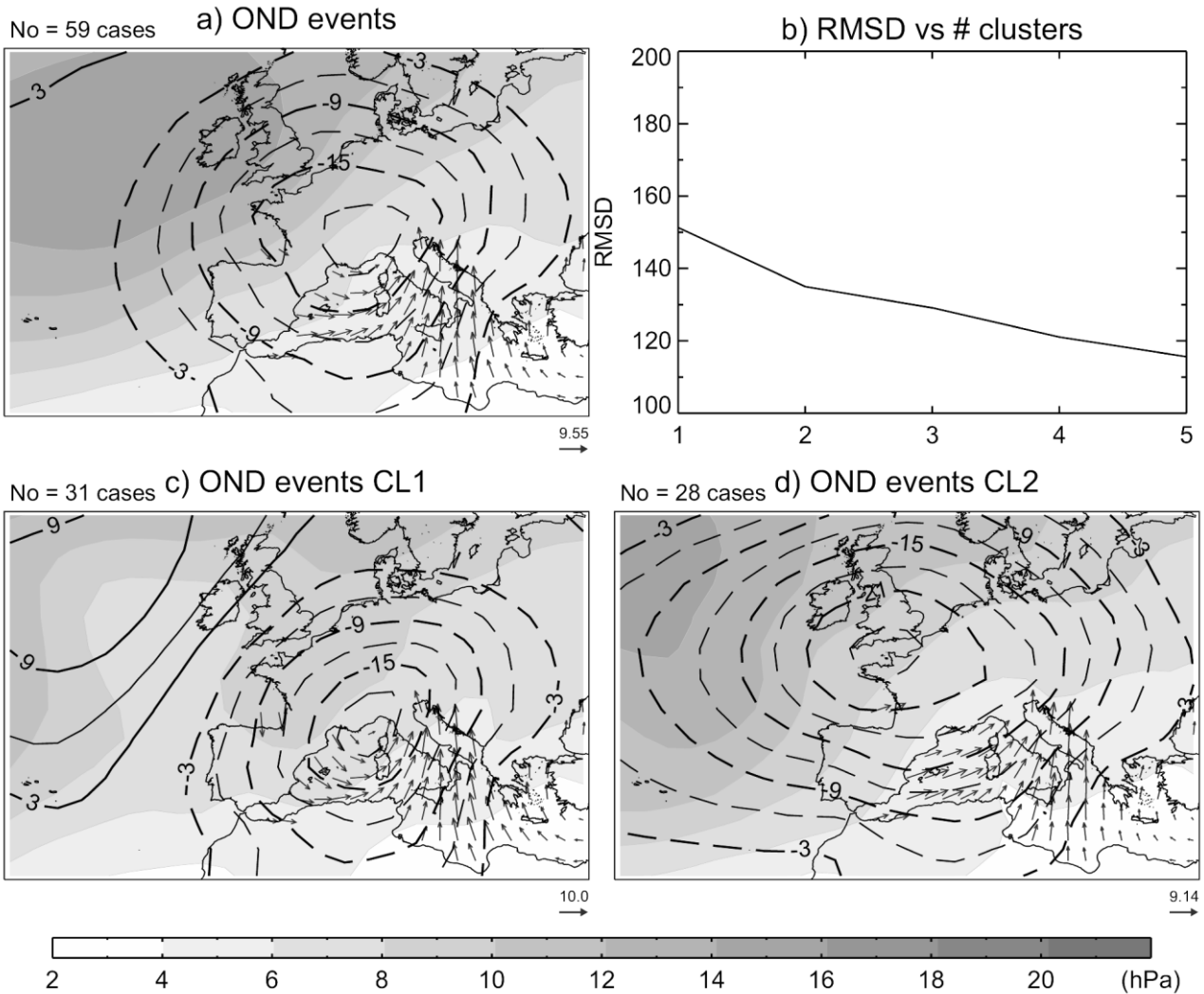
1144

1145

Figure 4-6 Density of tracks of cyclones (contour, measured as relative frequency of cyclones for each cell of 1.5 in%) based on ERA5 associated with storm surges with relative sea level higher than contributing to water-height maxima above 110 cm (relative frequency of cyclones for each cell of 1.5 in percentage of total, grey bar in the panel, based on ERA5). -Cyan tracks represent the events reported in Table 1 with relative sea level higher than water-height maxima-140 cm (see Table 1), the red, green and blue tracks represent is the track of Storm Vaia (29/10/2018, see Table 1), green line is the track of the event of 19/11/November 2019 2019, and 6/11/1966 events (the blue track is based on ERA40 data). Blue line is the track of cyclone producing the event of 4 November 1966 (based on ERA40 field). Yellow dot represents the location of the city of Venice while the blu,

1146  
1147  
1148  
1149

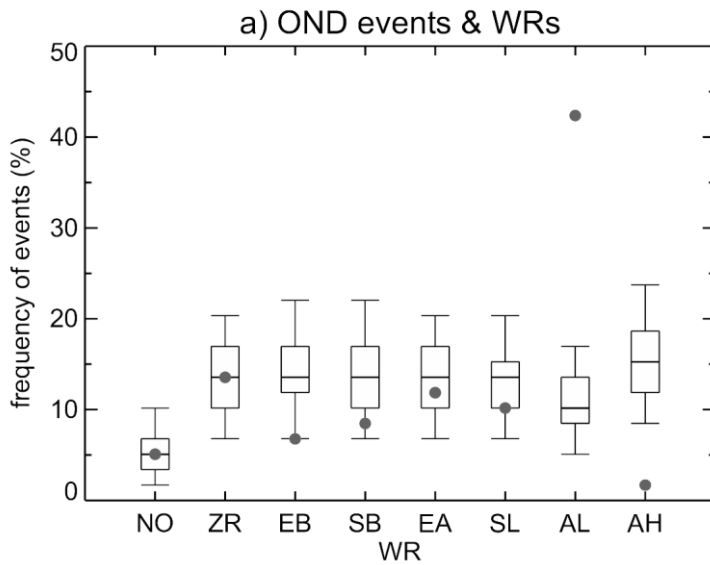
red and green dot represent the location of the storm of 4 November 1996, storm Vaia (29/10/2018) and that one associated with the event of November 2019.



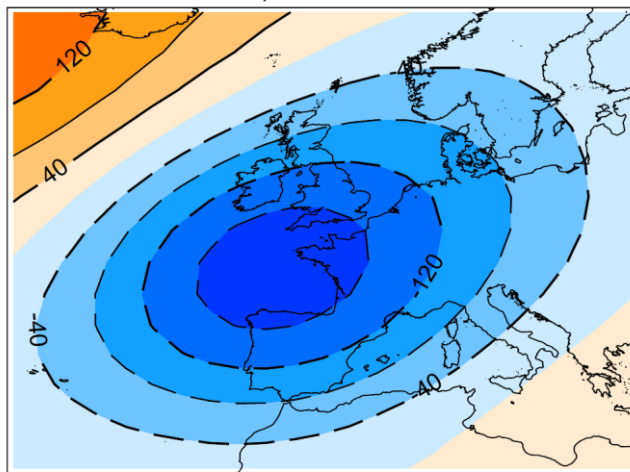
1150

1151  
1152  
1153  
1154  
1155  
1156  
1157  
1158  
1159  
1160

Figure 5a7 a) Composite of daily anomalies of sea level pressure (MSLP) over [30,60]°N, [30°W,30°E] (contours, hPa) and 10 m wind vector over the Mediterranean sea (arrows,  $\text{m s}^{-1}$ ) for ~~autumn-ND~~ **autumn-ND (October-November-December, OND) daily mean detrended water heights above the 99.5th surge events in Venice with surge height above the 99.5th percentile of the 1948-2018 distribution.** Shading shows the standard deviation of the composited MSLP fields. The number of cases is shown in the top left corner. The modulus of a reference wind speed vector is shown in the bottom right corner. Panel b) Root mean squared difference (RMSD) of the daily standardized anomalies of MSLP and 10 m wind vector as a function of the number of clusters. RMSDs are computed with respect to the centroid of the respective cluster; Panels c, d) as a) but when surge events are split in two groups, referred to as cluster one (CL1) and two (CL2), which correspond to the choice of two clusters in b). Note that a) is equivalent to considering one cluster with all events. Data sources: NCEP/NCAR reanalysis (Kalnay et al. 1996) and Fabio Raicich (Raicich 2015)

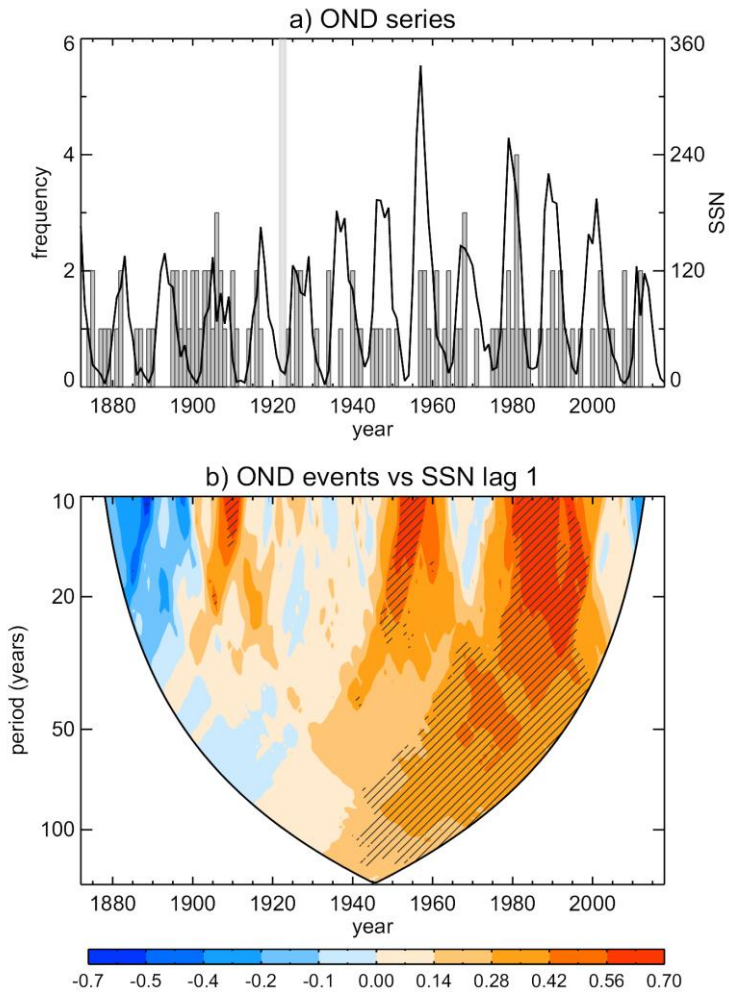


b) OND AL



1161

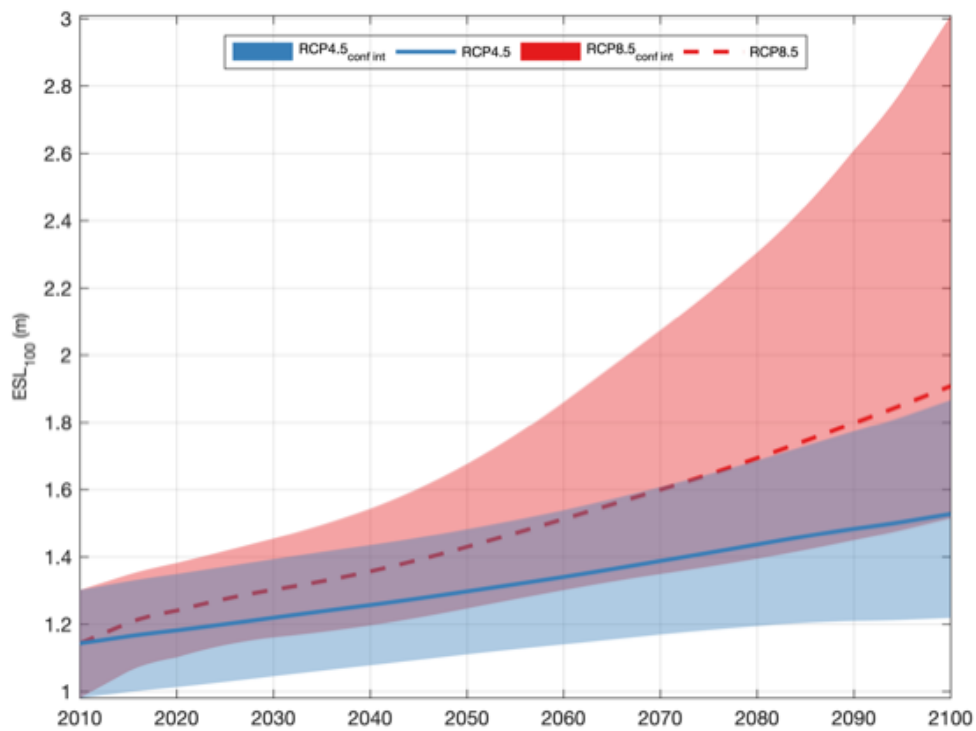
1162 Figure 6-8. Top panel: Relative frequency of autumn extreme daily mean detrended water heights above the 99.5th percentile  
 1163 of the surge events in Venice for 1948-2018 (in % with respect to the total number of events) occurring under the given Weather  
 1164 Regime (WR). Whiskers denote the random distributions obtained from a bootstrap of 5000 trials, each one containing the  
 1165 same number of autumn days of the 1948-2018 period as surge events. Boxes denote the inter-quartile distribution, with the  
 1166 median in between, and bars extend from the 5th to the 95th percentile of the random distributions. Surge events are defined  
 1167 as those with surge height above the 99.5th percentile of the 1948-2018 distribution. WRs are defined from daily fields of  
 1168 geopotential height at 500 hPa of the NCEP/NCAR reanalysis over the Euro-Atlantic sector [30, 65]°N, [30°W, 25°E]. Acronyms  
 1169 stand for: NO: No<sub>2</sub>- (i.e. undefined) WR; ZR: Zonal Regime; EB: European Blocking; SB: Scandinavian Blocking; EA: East  
 1170 Atlantic; SL: Scandinavian Low; AL: Atlantic Low; AH: Atlantic High. See Garrido-Pérez et al. (2019) for further details.  
 1171 Bottom panel: The AL pattern which-that is associated to the occurrence of more than 40% of extreme surges. -Data sources:  
 1172 NCEP/NCAR reanalysis (Kalnay et al. 1996) and Fabio Raicich (Raicich 2015).



1174

1175 **Figure 7-9 top panel: Time series of the autumn frequency of independent RSL extremes daily mean detrended**  
 1176 **water height (SEs) (IDMWH) extremes for 1924-2018, defined as daily peaks above the 99.5th percentile (35.0**  
 1177 **cm) of the total distribution for med by the RSL values of all-year days of the period 1924-2018. Daily peaks are**  
 1178 **required to be separated by more than 72h. Black line shows the autumn mean time series of the SunSpot Number**  
 1179 **(SSN). Bottom panel: Rank Spearman's ( $\rho$ ) correlations between the autumn frequency of independent daily**  
 1180 **mean detrended water-height extremes autumn frequency of surge events in Venice and the recently revised**  
 1181 **Sunspot Number (SSN) for running windows of different width (y-axis) entered/centred at each year of the 1872-**  
 1182 **2018 period (x-axis). Hatching denotes statistically significant correlations ( $p < 0.05$ ). Correlations are only**  
 1183 **computed when the sample size is equal or larger than 10 and it exceeds the half size of the window. The panel b)**  
 1184 **shows the correlation pattern maximizes for SSN leading by 1-yr, which produces the largest values. Data sources:**  
 1185 **WDC-SILSO, Royal Observatory of Belgium, Brussels (see Clette et al. 2014) and Raicich (2015). This figure**  
 1186 **follows the same approach adopted in Barriopedro et al. (2010), which considered the much shorter 1948-2008**  
 1187 **period and the frequency of meteorological surge extremes.**

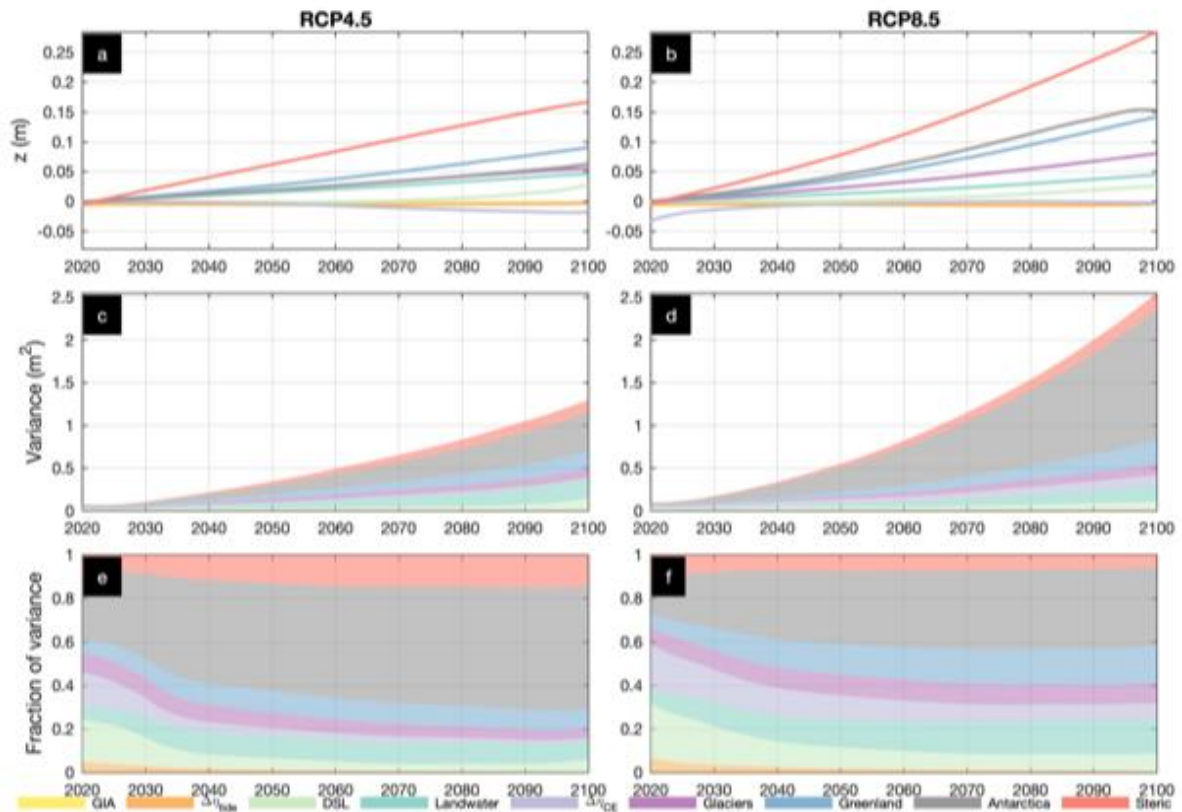
1188



1189

1190 **Figure 8-10** Time evolution of the 100y-ESL in the North-West Adriatic Sea : Time-series of the 100y-ESL under  
 1191 RCP4.5 (blue) and RCP8.5 (red). Lines show the corresponding medians and coloured areas. Heavy: median,  
 1192 patches express the 5th-95th percentiles (very likely range). This figure follows the same graphic format and it is  
 1193 based on the same simulations shown in Vousdoukas et al (2017), but it specifically refers to the area marked with  
 1194 the red box in figure 1, panel a.

1195



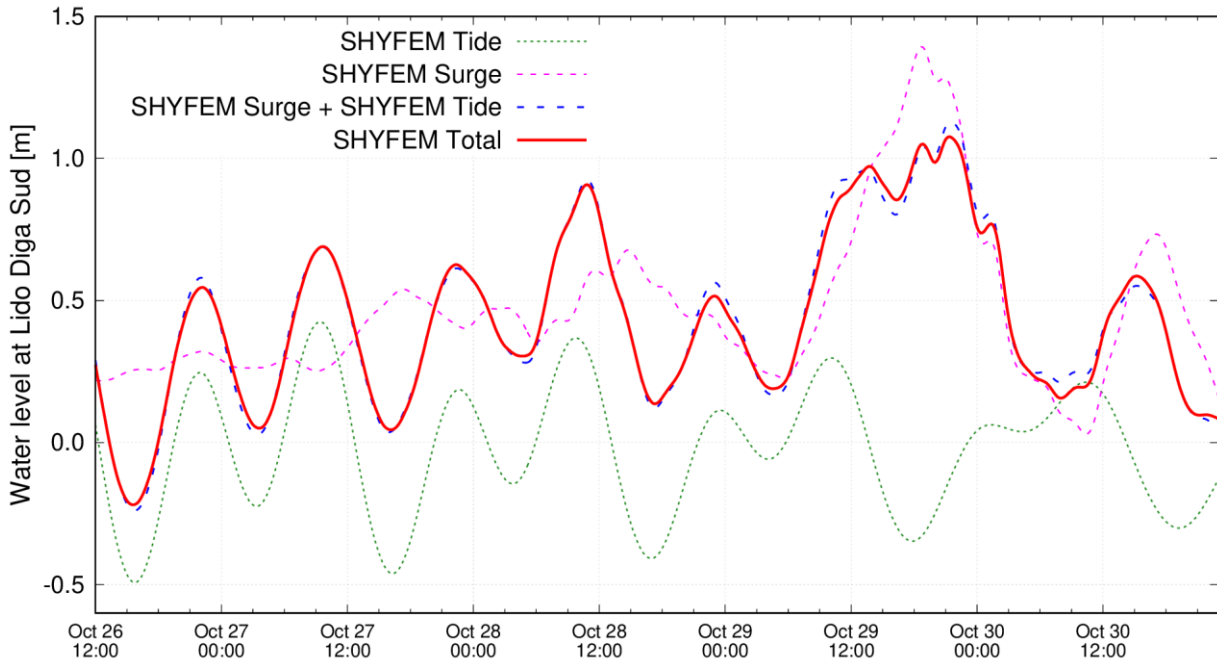
1197

1198 **Figure 9-11** Break-down of projected 100y-ESL contributions in the North-West Adriatic Sea and of their  
 1199 uncertainty, under RCP4.5 (a, c, e) and RCP8.5 (b, d, f). Projected increase of the 100y-ESL (with respect to the  
 1200 2001-2020 baseline) from changes in climate extremes, the high tide water level, as well as from SLR contributions  
 1201 from Antarctica, land-water, Greenland, glaciers, dynamic sea level (DSL), glacial isostatic adjustment (GIA), and  
 1202 steric-effects (a, b); variance (in m<sup>2</sup>) in components (c, d) and fraction of components' variance in global 100y-  
 1203 ESL change. Colors represent different components as in the legend and values express the global mean of the  
 1204 median. This figure follows the same graphic format and it is based on the same simulations shown in Vousdoukas  
 1205 et al (2018), but it specifically refers to the area marked with the red box in figure 1, panel a.

1206

1207

1208



1209

1210

1211

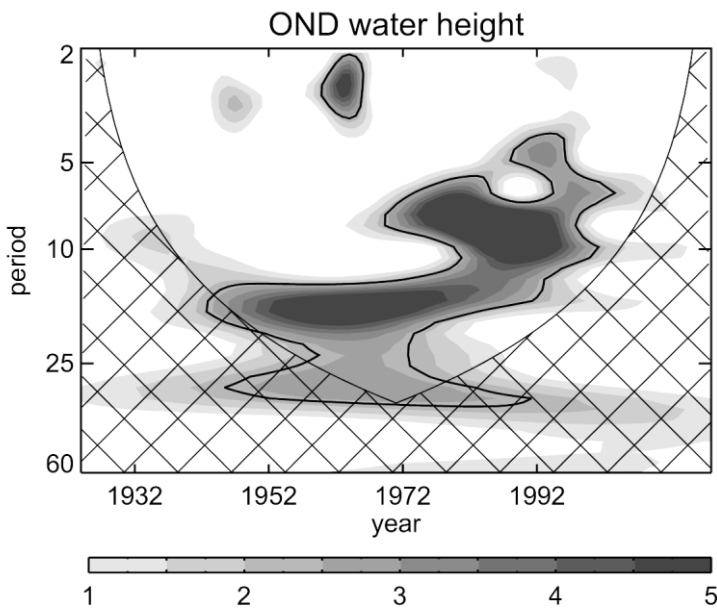
1212

1213

1214

1215

**Figure B1 Simulation of the event A.8 described in Appendix 1 performed with the SHIFEM model (see Cavaleri et al., 2019) for details. The different curves represent the model results using only the astronomical tidal forcing (SHYFEM Tide), the meteorological forcing (SHYFEM Surge) and the full forcing (SHYFEM Total). The dashed line (SHYFEM Surge + SHYFEM Tide) is the algebraic sum of the SHYFEM Tide and SHYFEM Surge results.**



1216

1217

1218

1219

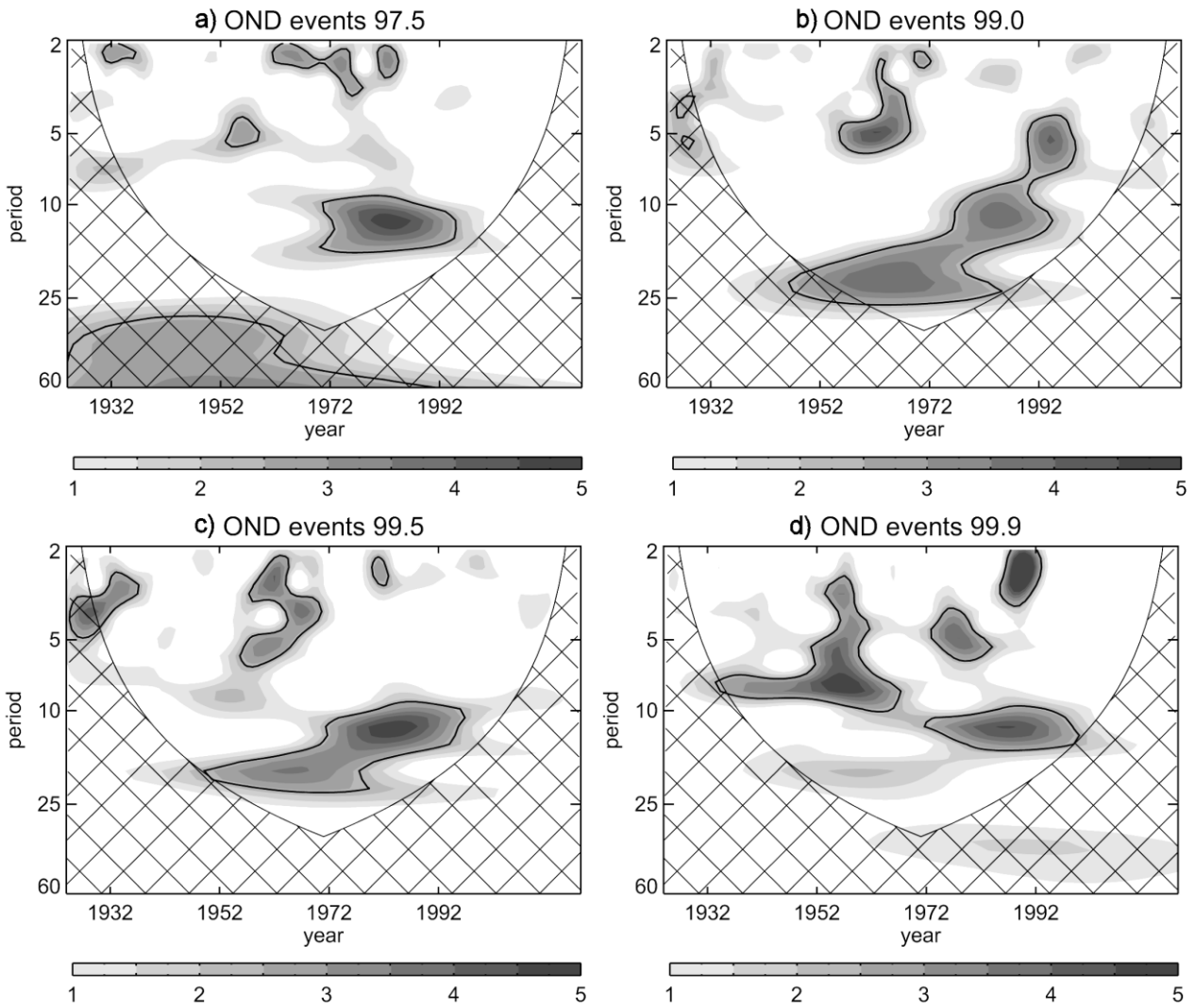
1220

1221

1222

1223

**Figure A.1-C1 Wavelet of time series of the autumn (October-November-December) mean time-series of Relative Sea Level (RSL water height) for 1924-2018, -expressed as power values normalized by the variance. Seasonal values are obtained from monthly means of the daily series. All months of this period have less than 10% missing days. Significant power density at 90% confidence level is highlighted by contours. This figure follows the same approach adopted in Barriopedro et al. (2010), which considered the much shorter 1948-2008 period.**



1224

1225

1226

1227

Figure A-C22- As figure [HI-1A.2](#) but for the autumn frequency series of daily independent SEs-detrended water heights above the 97.5th, 99th , 99.5th and 99.9th percentiles. This figure follows the same approach adopted in Barriopedro et al. (2010), which considered the much shorter 1948-2008 period and hourly data.



Datetime [UTC]	Water Height	Astronomical Tide	Seiche	Storm surge	Meteotsunami + MAV setup	PAW surge	IDAS	RSL (19y running mean)	Meteorological Surge	Detrended water height
Level (cm)										
1936-04-16 20:35:00	147	21	15	63	2	26	10	10	91	127
1951-11-12 07:05:00	151	43	1	44	3	39	6	15	86	130
1960-10-15 06:55:00	145	31	4	63	3	11	13	20	77	112
1966-11-04 17:00:00	194	-12	22	107	16	20	20	21	143	153
1968-11-03 06:30:00	144	35	10	47	2	21	7	22	70	115
1979-02-17 00:15:00	140	34	-2	39	8	26	13	22	73	105
1979-12-22 08:10:00	166	17	15	77	15	14	6	22	106	138
1986-02-01 03:00:00	159	30	22	48	4	18	15	22	70	122
1992-12-08 09:10:00	142	42	8	30	2	34	3	23	66	116
2000-11-06 19:35:00	144	16	7	69	1	17	8	26	87	110
2002-11-16 08:45:00	147	44	-8	47	1	22	14	27	70	106
2008-12-01 09:45:00	156	36	22	41	1	20	6	30	62	120
2009-12-23 04:05:00	143	20	32	22	4	18	16	31	44	96
2009-12-25 03:00:00	145	30	23	21	3	21	16	31	45	98
2010-12-24 00:40:00	144	35	2	39	3	22	12	31	64	101
2012-11-01 00:40:00	143	20	1	54	1	27	9	31	82	103
2012-11-11 08:25:00	149	47	-4	63	2	2	8	31	67	110
2013-02-11 23:05:00	143	38	14	39	0	6	15	31	45	97
2018-10-29 13:40:00	156	25	2	50	12	29	4	34	91	118
2018-10-29 19:25:00	148	-31	24	75	13	29	4	34	117	110
2019-11-12 21:50:00	189	36	5	42	37	21	14	34	100	141
2019-11-13 08:30:00	144	48	4	14	7	23	14	34	44	96
2019-11-15 10:35:00	154	47	4	25	2	27	15	34	54	105
2019-11-17 12:10:00	150	34	0	35	10	22	15	34	67	101
2019-12-23 08:45:00	144	39	39	6	1	14	11	34	21	99
Percentage (%)										
1936-04-16 20:35:00	147	14	10	43	1	18	7	7	62	86
1951-11-12 07:05:00	151	28	1	29	2	26	4	10	57	86
1960-10-15 06:55:00	145	21	3	43	2	8	9	14	53	77
1966-11-04 17:00:00	194	-6	11	55	8	10	10	11	74	79
1968-11-03 06:30:00	144	24	7	33	1	15	5	15	49	80
1979-02-17 00:15:00	140	24	-1	28	6	19	9	16	52	75
1979-12-22 08:10:00	166	10	9	46	9	8	4	13	64	83
1986-02-01 03:00:00	159	19	14	30	3	11	9	14	44	77
1992-12-08 09:10:00	142	30	6	21	1	24	2	16	46	82
2000-11-06 19:35:00	144	11	5	48	1	12	6	18	60	76
2002-11-16 08:45:00	147	30	-5	32	1	15	10	18	48	72
2008-12-01 09:45:00	156	23	14	26	1	13	4	19	40	77
2009-12-23 04:05:00	143	14	22	15	3	13	11	22	31	67
2009-12-25 03:00:00	145	21	16	14	2	14	11	21	31	68
2010-12-24 00:40:00	144	24	1	27	2	15	8	22	44	70
2012-11-01 00:40:00	143	14	1	38	1	19	6	22	57	72
2012-11-11 08:25:00	149	32	-3	42	1	1	5	21	45	74
2013-02-11 23:05:00	143	27	10	27	0	4	10	22	31	68
2018-10-29 13:40:00	156	16	1	32	8	19	3	22	58	76
2018-10-29 19:25:00	148	-21	16	51	9	20	3	23	79	74
2019-11-12 21:50:00	189	19	3	22	20	11	7	18	53	75
2019-11-13 08:30:00	144	33	3	10	5	16	10	24	31	67
2019-11-15 10:35:00	154	31	3	16	1	18	10	22	35	68
2019-11-17 12:10:00	150	23	0	23	7	15	10	23	45	67
2019-12-23 08:45:00	144	27	27	4	1	10	8	24	15	69
AVERAGE		20	7	30	4	14	7	18	48	75

1228  
1229  
1230  
1231  
1232  
1233  
1234  
  
1235

**Table 1 List of the extreme sea-levels higherwater heights (higher than 140 cm) alongside the contributions (see section 2.1 and 2.2): astronomical tide, seiches, storm surge, meteotsunami and local Mesoscale Atmospheric Variability (MAV) set-up, PAW surge, IDAS variability, Relative Mean Sea Level, meteorological surge and total surge. All values in cm. The Relative Mean Sea-levelwater-height values are anomaly-referenced to the 'Zero Mareografico Punta Salute' (ZMPS). The upper panel shows the actual values (cm), the lower panel the percentage (%) of each contribution.**

Date	MaxWH (cm)	Sources
1966-11-04	194	DO68, CA01, BC06, CPSM
2019-11-12*	189	ISP20
1979-12-22	166	CA01, BC06, CPSM
1986-02-01	159	CA01, BC06, CPSM
2018-10-29*	156	BC06, ISPRA, CPSM
2008-12-01	156	BC06, ISPRA, CPSM
2019-11-15	154	CPSM
1951-11-12	151	DO61, CA01, BC06, CPSM
2019-11-17	150	CPSM
2012-11-11	149	BC06, ISPRA, CPSM
2018-10-29*	148	BC06, ISPRA, CPSM
2002-11-16	147	BC06, CPSM
1936-04-16	147	DO61, BC06, CPSM
2009-12-25	145	BC06, CPSM
1960-10-15	145	DO61, CA01, BC06, CPSM
2019-12-23	144	ISP19
2019-11-13*	144	CPSM
2010-12-24	144	BC06, ISPRA, CPSM
2009-12-23	144	BC06, CPSM
2000-11-06	144	CA01, BC06, CPSM
1968-11-03	144	CA01, BC06, CPSM
2013-02-12	143	BC06, ISPRA, CPSM
2012-11-01	143	BC06, ISPRA
1992-12-08	142	CA01, BC06, CPSM
1979-02-17	140	ISP19

1236

1237

1238

1239

1240

1241

**Table A-1** List of the surge events higher than 100 cm alongside the respective water-height maxima. The asterisk indicates the two RSL peaks during the same event on 29 October 2018. (AN41 = Annali, 1941; CA01 = Canestrelli et al., 2001; CA19 = Cavaleri et al., 2019, CA20 = Cavaleri et al., 2020, CPSM = CPSM, 2020; DE06 = de Zolt et al., 2006; DO61 = Dorigo, 1961b; DO68 = Dorigo, 1968; ISPRA = ISPRA, 2008-2018; ISPRA/CPSM/CNR = ISPRA et al., 2020)